

NASA Technical Memorandum 4109

Updated Users' Guide for TAWFIVE With Multigrid

N. Duane Melson and Craig L. Streett
Langley Research Center
Hampton, Virginia

NASA

National Aeronautics and
Space Administration

Office of Management

Scientific and Technical
Information Division

1989

Contents

Summary	1
Introduction	1
Engineering Aspects	1
Viscous-Inviscid Interaction Theory	1
Inviscid Method	2
Boundary-Layer Method	3
Lift Specification	3
Sample Results	4
Users' Guide	4
Input Description	4
Geometric data	5
Inviscid-iteration and global-interaction control parameters	6
Restart data	6
Interaction strategy	6
Output Description	8
References	9
Tables	11
Figures	59

PRECEDING PAGE BLANK NOT FILMED

Summary

A program for the Transonic Analysis of a Wing and Fuselage with Interacted Viscous Effects (TAWFIVE) has been developed. A brief discussion of the engineering aspects of the program is included. Descriptions of recent improvements (multigrid acceleration and a lift specification option) are given. A general discussion of the input data, program output, and strategies for running the program is given, and tables and figures giving detailed definitions of the input data are included to aid in the preparation of data sets.

Introduction

In recent years, research has produced significant improvements in the mathematical modeling of transonic flow fields over increasingly complex configurations. The first calculations of transonic flow about simple airfoils were performed in the early 1970's using a nonconservative formulation of the potential equation (refs. 1 and 2). In the last half of the decade, computational abilities progressed up to the point where flows around wing and wing-body configurations could be calculated using inviscid, conservative, full-potential formulations. Some of the calculations for wing-alone configurations also included two-dimensional, strip boundary-layer corrections. The program described in reference 3 added to the progression of increasing computational capabilities by providing the ability to model flows for a wide class of transport-type wing and fuselage configurations using a conservative, finite-volume, potential flow solver interacted with a three-dimensional (3-D) boundary-layer method. The present work adds affordability to this line of progression by significantly reducing the computational work required to obtain accurate solutions. This was accomplished by replacing the original successive line overrelaxation (SLOR) inviscid method (FLO30) with a multigrid accelerated method (FLO30M).

Although more complex Euler and Navier-Stokes methods are currently available (see, for example, refs. 4-8), the cost of these methods can be prohibitively high for design work. For transport configurations at cruise conditions, the potential approximation interacted with a 3-D boundary-layer calculation gives sufficiently accurate solutions for design work. With the use of multigrid acceleration in the iterative solution of the potential equation and the use of the integral-form boundary-layer equations, the cost of calculations can be quite low. With the present method, convergence to engineering accuracy can be obtained for lifting transonic configurations in less than 10 minutes central

processing unit (CPU) time on a CRAY-2 supercomputer (manufactured by Cray Research, Inc.).

A new capability allowing the specification of lift, rather than angle of attack, has been developed. This technique was not available in earlier versions.

Engineering Aspects

The program described in this report is called TAWFIVE, an acronym for Transonic Analysis of a Wing and Fuselage with Interacted Viscous Effects. It was developed at the NASA Langley Research Center. Important points about TAWFIVE are summarized in this section. Details about recent improvements to the program are also given.

Viscous-Inviscid Interaction Theory

At high Reynolds numbers N_{Re} , the Navier-Stokes equations are a so-called singular perturbation problem. That is, the second-order (viscous) terms are important only in a thin region near a solid surface. Thus, asymptotic theory can be used to simplify the solution process by breaking the problem into a loosely coupled set of modified equations, one valid in the "outer" region and the other valid in the "boundary layer." The thickness of this layer is $O(N_{Re}^{-1/2})$ for laminar flow and $O(\ln N_{Re})$ for turbulent flow (ref. 9). In the outer region, the first-order asymptotic equations are the standard inviscid equations (potential or Euler), whereas the usual Prandtl boundary-layer equations are valid in the boundary region. The equations are coupled by modified surface boundary conditions for the inviscid equation; one choice is that the usual flow-tangency conditions are imposed at a location displaced outward from the wall. This "displacement thickness" comes from the solution of the inner (boundary-layer) equations and corresponds physically to the fact that the boundary layer is mass deficient relative to the free stream. The pressure to first-order accuracy is determined asymptotically by the solution of the outer (inviscid) equations.

This theory presumes that there are no large gradients/small scales in any direction other than normal to the surface. Thus, it is strictly valid only in regions away from separation/reattachment, normal shocks, trailing edges, or wingtips. The neglect of these so-called strong-interaction regions has generally been found to not greatly affect the overall results for the cases considered here.

As with essentially all viscous-inviscid interacted calculation methods, what is sought here is a self-consistent solution of the coupled inviscid outer equations and boundary-layer inner equations, rather than a rigorous, matched asymptotic expansion.

This self-consistent set of solutions is obtained iteratively. In the present method, the outer inviscid flow is modeled using the conservative formulation of the full-potential equation. The inner viscous flow is modeled on the wing using the three-dimensional, integral boundary-layer equations. The interaction process starts with a solution of the outer flow field. Pressures are computed at the wing surface and are used to calculate the boundary layer. The boundary-layer displacement thickness is then computed and added normal to the surface of the "hard" geometry. This new displaced wing surface is then regridded and the inviscid flow field is recomputed. New values of the inviscid pressures are then used by the boundary-layer method to predict a new displacement thickness distribution. An underrelaxed update of the previously predicted displacement thickness is then made to obtain a new displacement thickness correction that is added to the "hard" geometry. These global iterations (inviscid solution plus boundary-layer calculation) are continued until suitable convergence is obtained.

Inviscid Method

The outer inviscid flow is modeled by a conservative, finite-volume, full-potential method based on the multigrid program FLO30M (ref. 10) developed by Caughey. (Ref. 10 should be consulted for complete details, but a short summary is presented below.)

If the simplifying assumptions of inviscid, irrotational flow are made, the Navier-Stokes equation can be reduced to the full-potential equation. For transonic flows with weak shocks, the assumption of irrotational flow is reasonably accurate. After Caughey (ref. 10), the conservative potential equation in Cartesian coordinates (x, y, z) is

$$(\rho\phi_x)_x + (\rho\phi_y)_y + (\rho\phi_z)_z = 0 \quad (1)$$

where ρ is the density and ϕ is the velocity potential. Since the flow is isentropic, the density is a function only of γ (the ratio of specific heats), M_∞ (the free-stream Mach number), and q (the local velocity magnitude).

In FLO30M (and subsequently TAWFIVE), a generalized transformation to a boundary-fitted coordinate system X, Y, Z is made. The Jacobian matrix of the transformation is

$$\mathbf{H} = \begin{bmatrix} x_X & x_Y & x_Z \\ y_X & y_Y & y_Z \\ z_X & z_Y & z_Z \end{bmatrix} \quad (2)$$

Equation (1) can then be rewritten as

$$(\rho h U)_X + (\rho h V)_Y + (\rho h W)_Z = 0 \quad (3)$$

where h is the determinant of \mathbf{H} , and U, V , and W are the contravariant velocity components.

A fully conservative, finite-volume approximation of equation (3) is made. Within each finite-volume cell, a trilinear variation of each of the dependent and independent variables is assumed. Details of this are found in reference 10. The assumption of trilinear variation is used to determine ρ, h, U, V , and W at the center of each cell. A set of auxiliary cells are defined whose faces lie midway between the faces of the primary cells. Conservation of the fluxes across the faces of the auxiliary cells is imposed to satisfy equation (3). Because of the one-point integration scheme used to evaluate the fluxes, the solution of odd- and even-number points in the grid tends to be decoupled (ref. 10). Appropriate recoupling terms are added to improve the stability of the solution while maintaining second-order accuracy.

It is necessary to add explicit artificial viscosity in supersonic regions of the flow. This artificial viscosity is added in a manner that mimics the upwind bias in the original Jameson rotated difference scheme (ref. 2). This viscosity is added only when the local Mach number exceeds a specified critical Mach number. As a user option, the artificial viscosity can be reduced from second order to first order to stabilize solutions containing strong shocks.

A finite-volume grid is algebraically constructed about an arbitrary wing-fuselage combination. A C-H topology is used with C wrapped around the airfoil and H extending in the span direction. (See fig. 1.) An i, j, k scheme is used to structure the grid with the i -direction wrapped around the airfoil, the j -direction normal to the wing surface, and the k -direction out the span.

The resulting set of equations for the flux balances on the grid volumes are solved using the successive line overrelaxation (SLOR) method. Implicit lines are constructed along either the i - or j -direction. The implicit direction can be alternated between the i - and j -directions in the spirit of an alternating direction implicit (ADI) scheme. With second-order viscosity, the systems of equations are pentadiagonal matrices. The pentadiagonal inversion scheme is described in detail in reference 10.

Convergence in FLO30M is accelerated by the application of multigrid. Since the transonic potential equation is nonlinear, Full Approximation Storage (FAS) multigrid was used. More details on multigrid in general can be found in reference 11. A fixed V-cycle strategy was incorporated with a

specified number of subiterations performed between restrictions and a possibly different specified number of subiterations performed between prolongations. Volume-weighted averages in the computational space were used in the restrictions. Four-point Lagrangian interpolations were used in the prolongation operator. Specific details on the multigrid in FLO30M can be found in reference 10.

Boundary-Layer Method

To account for viscous effects, the TAWFIVE code uses first-order, weak, self-consistent interactions in the sense of Melnik et al. (ref. 12). The first-order effects of boundary-layer displacement on the wing surface and in the wake are included. Viscous effects on the body are ignored. Wake-curvature effects are currently not implemented. The reader is directed to references 13–18 for more detail.

The fully three-dimensional boundary layer on the wing is computed using a compressible integral method capable of computing either turbulent or laminar boundary layers, and the user specifies a fixed, constant-chord-fraction transition point from laminar to turbulent flow. The turbulent method was based on the work of Smith (ref. 16) with extensions (ref. 13), and the laminar method was developed by Stock (ref. 17). Small regions of separation are also modeled. Since transient regions of separated flow often occur during the initial stages of convergence in an interactive scheme, a simple constant-value extrapolation of the displacement thickness may be specified. This extrapolation is nonphysical but is a numerical aid to allow convergence to a nonseparated condition.

The initial condition for the boundary-layer calculation (near the leading edge) is provided by an attachment-line analysis. In the original TAWFIVE, it was necessary to specify this constant-chord-fraction starting location for both the upper and lower wing surfaces. The multigrid version of TAWFIVE contains logic that determines the appropriate value. The criteria used for this selection are: (1) the starting location must be aft of the stagnation point, and (2) the starting location must be in a region of favorable pressure gradient. These constraints must be satisfied by a single value suitable for all span locations. For wings with excessive twist, this may be impossible. Temporary retwisting of the wing may be necessary to start the solution process, or the starting value may be specified to override the logic and attempt to start the boundary-layer calculation in a region of a weak adverse pressure gradient.

Lift Specification

In aircraft design, it is often desired to match

the lift predicted by a computational tool with a prescribed value. The capability to input a value for lift into a two-dimensional potential equation solver and obtain a value for angle of attack has been available for years. A new method to prescribe wing lift in three-dimensional potential flow calculations is described below. This method does not include the fuselage lift. The method is relatively simple and can be retrofitted into existing three-dimensional potential solvers.

First, it is noted that the wing lift coefficient is the integral of the section lift coefficients over the semispan divided by the semispan:

$$C_L = \frac{\int_{\text{root}}^{\text{tip}} (C_l)_k dz}{z_{\text{tip}} - z_{\text{root}}} \quad (4)$$

where C_L is the wing lift coefficient, $(C_l)_k$ is the section lift coefficient at section k , and z is the span location measured from root to tip. Using trapezoidal integration to numerically evaluate the integral in equation (4) gives

$$C_L = \frac{1}{z_{\text{tip}} - z_{\text{root}}} \frac{1}{2} \sum_{k=1}^{k_{\text{tip}}-1} \left\{ [(C_l)_k + (C_l)_{k+1}] (z_{k+1} - z_k) \right\} \quad (5)$$

By definition,

$$C_l = \frac{l}{\frac{1}{2} \rho_{\infty} V_{\infty}^2 c}$$

where l is the section lift, ρ_{∞} is the free-stream density, V_{∞} is the free-stream velocity, and c is the section chord. From the Kutta-Joukowski law,

$$l = \rho_{\infty} V_{\infty} \Gamma$$

where Γ is the circulation. Combining these with equation (5) gives

$$C_L = \frac{1}{z_{\text{tip}} - z_{\text{root}}} \frac{1}{V_{\infty}} \sum_{k=1}^{k_{\text{tip}}-1} \left[\left(\frac{\Gamma_{k+1}}{c_{k+1}} + \frac{\Gamma_k}{c_k} \right) (z_{k+1} - z_k) \right] \quad (6)$$

In potential theory,

$$\Gamma_k = ([\phi]_{\text{te}})_k + \Delta y_k V_{\infty} \sin \alpha$$

where $([\phi]_{\text{te}})_k$ is the jump discontinuity in the potential at the trailing edge (te) at section k , Δy_k is the distance between the discrete points used to evaluate $([\phi]_{\text{te}})_k$, and α is the free-stream angle of attack.

Therefore,

$$C_L = \frac{1}{z_{\text{tip}} - z_{\text{root}}} \frac{1}{V_\infty} \sum_{k=1}^{k_{\text{tip}}-1} \left\{ \left[\frac{([\phi]_{\text{te}})_{k+1}}{c_{k+1}} + \frac{([\phi]_{\text{te}})_k}{c_k} \right] (z_{k+1} - z_k) \right\} \\ + \frac{1}{z_{\text{tip}} - z_{\text{root}}} \sin \alpha \sum_{k=1}^{k_{\text{tip}}-1} \left[\left(\frac{\Delta y_{k+1}}{c_{k+1}} + \frac{\Delta y_k}{c_k} \right) (z_{k+1} - z_k) \right] \quad (7)$$

For simplicity, let

$$A' = \frac{1}{z_{\text{tip}} - z_{\text{root}}} \sum_{k=1}^{k_{\text{tip}}} \left\{ \left[\frac{([\phi]_{\text{te}})_{k+1}}{c_{k+1}} + \frac{([\phi]_{\text{te}})_k}{c_k} \right] (z_{k+1} - z_k) \right\}$$

and

$$B' = \frac{1}{z_{\text{tip}} - z_{\text{root}}} \sum_{k=1}^{k_{\text{tip}}} \left[\left(\frac{\Delta y_{k+1}}{c_{k+1}} + \frac{\Delta y_k}{c_k} \right) (z_{k+1} - z_k) \right]$$

Substitution in equation (7) gives

$$C_L = \frac{1}{V_\infty} A' + B' \sin \alpha$$

In the present method, velocities are nondimensionalized by the free-stream velocity. Therefore, $V_\infty = 1$,

$$C_L = A' + B' \sin \alpha \quad (8)$$

and

$$\alpha = \sin^{-1} \left(\frac{C_L - A'}{B'} \right) \quad (9)$$

The lift coefficient based on equation (8) is relatively cheap to calculate. It is a useful parameter to help monitor convergence of lifting cases when the angle of attack is specified.

When the lift-specification mode is used, the values of $([\phi]_{\text{te}})_k$ are calculated by the flow field solver in the same way as they are in alpha-specification mode. These values and geometric quantities are then used to calculate A' and B' which are substituted into equation (9). The new value of α is used to update the angle of attack by underrelaxation.

Sample Results

A sample calculation for a typical transonic transport was performed. The configuration described in reference 19 as Pathfinder I was considered. A free-stream Mach number M_∞ of 0.82, an angle of attack α of 1.93° , and a Reynolds number N_{Re} of 17.0×10^6 were specified. An inviscid calculation was performed as well as a viscous calculation. A comparison with presently unpublished experimental data

provided by P. F. Jacobs of the Langley Research Center is shown in figure 2 for six different span stations η over a range of pressure coefficients C_p . Note that the inviscid calculation does a poor job of predicting the shock strength and location, especially near the tip. With the viscous effects added, the shock moves forward and its strength is reduced. The error in both the inviscid and viscous solutions near the root is attributed to the midwing configuration used for the computations, whereas the experimental data were obtained for a low-wing configuration. (The low-wing configuration caused gridding problems.) The agreement of the viscous results with the experimental data is quite good except at the root and tip. The results were obtained with 10 global iterations in less than 7.5 minutes CPU time on a CRAY-2.

The calculations for the Lockheed wing A performed in reference 13 with the original TAWFIVE were repeated with the new multigrid TAWFIVE. The results were identical to those previously obtained and thus are not repeated here.

The Lockheed wing A case was then used to demonstrate the lift specification capability. A value of C_L of 0.4 was specified for $M_\infty = 0.5$ and $N_{Re} = 2.2 \times 10^6$ with a starting angle of attack of 1.0° . The solution was converged after six global iterations with an angle of attack of 2.36° and a value of C_L based on the circulation equal to 0.4000. The lift coefficient based on the integrated pressures was 0.4073, which agrees within 2 percent of the specified lift and the lift based on the circulation.

Users' Guide

Input Description

The input to TAWFIVE is limited to geometric definition of the configuration, free-stream flow quantities, and iteration control parameters. The geometric input consists of the definition of a series of airfoil sections to define the wing and a series of fuselage cross sections to define the fuselage. The wing may have an arbitrary airfoil shape that may change with span location. Because of grid limitations in the inviscid outer-flow calculations, the wing cannot have large amounts of taper or sweep. High-aspect-ratio wings are modeled more accurately than low-aspect-ratio wings since no special provisions are made to accurately model the wing-fuselage juncture or the wingtip region. Boundary-layer theory is not valid in the wing-fuselage juncture region or in the wingtip region. The fuselage may have an arbitrary shape. With the proper choice of input options, a simple, circular cross section may be used for the fuselage or an arbitrary cross-section shape may be defined

by reading coordinate pairs. The fuselage may be closed at both ends, a circular sting may extend to either upstream or downstream infinity, or both. The program finds the wing-fuselage intersection by linear extrapolation of the wing surface to the fuselage surface.

A general description of the input necessary to run the TAWFIVE program is provided in the text below. Detailed descriptions of each of the input variables are given in the tables at the end of the report. Once the user is familiar with the program, the tables should provide sufficient information to prepare input. For first-time users, sample input files are also included as tables at the end of the report. The input for TAWFIVE is divided into three areas: (1) geometric data, (2) inviscid-iteration and global-interaction control parameters, and (3) restart data. Each of these three areas is read from different tape units. (See table 1.)

For users familiar with the original TAWFIVE, the following points are noted. The geometric input is identical to the original TAWFIVE, whereas the inviscid-iteration and global-interaction control parameters have been changed to account for the input necessary to control the multigrid acceleration and the lift specification capability. The restart data are not compatible with the original code since more grid points lie on the wing with the multigrid code than with the original code. (There are 25 points in the span direction versus only 21 points in the original code.)

Geometric data. The geometric data are read from unit 7 and include the definition of the wing and fuselage. The wing should have a high aspect ratio and a limited taper ratio and sweep angle. The wingtip is not modeled accurately enough to allow the analysis of wings with very low aspect ratio, and grid problems are encountered for high taper ratio or sweep angle. Since problems with aspect ratio, taper ratio, and sweep angle may be cumulative, it is impossible to give specific limits on each. In general, the program performs best for configurations similar to conventional transports.

The wing is defined by the input of successive airfoil-section shapes ordered from the wing root to the tip. A minimum of two airfoil sections is required to define the wing. Up to 21 airfoil sections may be input to define complex wing geometries. All input airfoil sections must have the same number of defining coordinate pairs, and the points must be at the same percent chord locations for all the sections. A high-definition, smooth leading-edge input is important. At least five defining points

should be ahead of the chord fraction equal to one-half the leading-edge radius.

The location of the first wing section at the root of the wing is very critical. The root section must be defined as close as possible to the wing-fuselage intersection. However, it should be defined outside the fuselage, since linear extrapolation along the wing surface is used to determine the wing-fuselage intersection.

The wing airfoil-section data are used to generate a well-defined "hard" surface used internally in the program to apply the boundary-layer displacement thickness corrections. This internal hard surface consists of the input airfoil sections and optional additional stations created using linear lofting between the input airfoil sections. The number of sections added between each of the defining sections is an input. The internal hard-surface strategy is used to reduce the amount of data necessary to define the wing surface while retaining a sufficient number of points for application of the boundary-layer correction. The number of input airfoils plus the number added by linear lofting must not exceed 21.

The fuselage is defined by the input of successive cross-section definitions ordered from the nose of the fuselage to the tail. A maximum of 25 cross sections may be read to define an arbitrarily shaped fuselage. An optional circular fuselage is available that requires significantly less input. With either the arbitrary or the circular fuselage, circular cylinders extending to upstream infinity or downstream infinity, or both, may be used.

The relative placement of the wing and fuselage is described through the combination of the fuselage cross-section definitions and the location of the wing airfoil-section leading-edge points. It is important to note that the fuselage station locations, their defining coordinates, and the wing airfoil-section leading-edge-point locations and their chord lengths must all be in the same units. The wing airfoil-section coordinates may be in whatever units are convenient since they are normalized and then are scaled by the input section chord length, shifted by the leading-edge location, and rotated by the section angle of attack.

Detailed definitions of the geometry input variables are given in table 2, which utilizes figures 3-5, and a sample data set is given in table 3. In general, each of the data record images is preceded by a descriptive record that simply lists the variable names. These descriptive records are either read with a character format and stored in a dummy array or the record is just skipped. Either way, whatever appears on the descriptive records is not used by the program. The records are in the data set to aid in the interactive preparation of the input file. This same

format (a descriptive record followed by a data record) is also used for the input of the inviscid-iteration and global-interaction control parameters. All geometric data and iteration and interaction control inputs on these two files are real numbers; no integer formats are used.

Inviscid-iteration and global-interaction control parameters. The inviscid-iteration control parameters and the inviscid/boundary-layer interaction control parameters are read from unit 5. (See table 1.) These inputs contain a block of information that is repeated for each global iteration. Although the repetition of these blocks could have been eliminated with a global-iteration control variable, this would have removed the flexibility of independently changing the parameters from one global iteration to the next. Within each block are three sections:

The first section is read by 11 read orders in the inviscid part of the code. (A read order is a read statement in the program or an order to read.) The first read order is for the title of the global iteration. The second and third read orders are for inviscid grid and artificial viscosity parameters. The fourth and fifth are for inviscid output, inviscid initial condition, and boundary-layer correction parameters. The sixth through ninth define inviscid-iteration control parameters, and the tenth and eleventh give free-stream flow and lift specification parameters.

The second section within each block contains input information read by the boundary-layer and wake-treatment part of the program. This section contains five read orders. The first read order reads a two-record title. The second and third read orders contain the data for the boundary-layer calculation, and the last two read orders contain the lag-entrainment flag and boundary-layer print-control parameter.

The third section within each block of input data contains variables that control the interpolation of the boundary-layer information from the boundary-layer grid points to the wing hard-surface coordinate points. There are only two read orders in this section.

The blocks of data containing the inviscid-data section, the boundary-layer/wake-data section, and the interpolation-data section are repeated for each of the global iterations. The boundary-layer-control parameter (BLCP) in the inviscid section is varied in the initial global iterations to control the boundary-layer and wake corrections made before each inviscid calculation. Blocks of input data are repeated and

global iterations are continued until terminated by the input of a value of zero for the variable FNX.

Details of the inviscid-iteration and global-interaction control variables are given in table 4. A sample data set is given in table 5. Since the inviscid portion of the calculation is performed by code that was based on FLO30, the input is similar to that described in reference 20.

Restart data. The restart data are read from unit 4 and are in unformatted binary form. The restart file is generated by the program and is written on unit 3. The file contains the three-dimensional array of potential values from the inviscid calculation as well as the one-dimensional array containing the values of the jump in the potential across the vortex sheet along the trailing edge of the wing. From the boundary-layer and wake calculations, the restart file also contains the two-dimensional array of displacement thickness on the wing and in the wake. Also in the restart file is the two-dimensional array containing the wake-momentum thickness.

The restart information is written by subroutine SAVE which is called in two places by the main program TAWFIVE. The file is rewound before the data are written in each call to SAVE. The first call to SAVE is after the inviscid calculation. The second call to SAVE is after the boundary-layer and wake calculations. These two calls make possible a restart of the calculation from the previous step if a problem develops in either the inviscid or viscous calculation. The message "DATA SAVED ON RESTART FILE" is written to unit 6 whenever subroutine SAVE has written the restart data.

The restart file is also used when a case is stopped before it is fully converged. Global iterations may be continued using the information on the restart file. The restart option is invoked when FCONT is set equal to 3.0.

Interaction strategy. As with all computational tools, there are two important objectives that must be considered when making calculations with TAWFIVE. The first and most important is the requirement that the iterations be stable and converge to the correct answer. It is also important that the converged solution be reached with the minimum amount of work. This section of the report is an attempt to outline some strategies that will help assure that the aforementioned criteria are satisfied.

TAWFIVE runs must begin with the calculation of the inviscid flow about the wing-fuselage configuration (BLCP = 0.0). To develop the flow quickly, grid refinement may be used. The use of grid refinement is not as critical with the new multigrid version of TAWFIVE as it was with the original version. The

initial calculation on the fine grid should not be allowed to converge very far since high gradients may develop that can cause problems with the boundary-layer calculations. These gradients will tend to be smoothed by viscous corrections.

After the initial inviscid calculation, the first boundary-layer calculation is performed. Based on this calculation, displacement thickness corrections should be made to the wing and wake. The boundary-layer transition point for the upper and lower surfaces should be set to zero, thus forcing the boundary layer to be purely turbulent. Since the turbulent scheme is more robust than the laminar one, this allows the program to get through the initial transient. The displacement thickness corrections should be underrelaxed ($RELI \approx 0.8$). For the first boundary-layer calculation, no previous values of displacement thickness are available for underrelaxation, and thus values of zero are used. Therefore, the calculated values of displacement thickness are effectively multiplied by the magnitude of the boundary-layer relaxation parameter ($RELI$) in the first global iteration.

The second inviscid calculation is then performed on a configuration where the wing and wake have been modified by the displacement thickness generated by the first boundary-layer calculation ($BLCP = 2.0$). Wake-curvature effects are not included. Since the displacement thickness can significantly change the shape of the wing, it is best to start the second inviscid calculation with the potential field reinitialized to free-stream conditions ($FCONT = 1.0$). Since the potential field is reinitialized, grid refinement may be used. The second boundary-layer calculation is then performed. From this calculation, displacement thickness corrections should be used on the wing and wake. Wake-curvature effects and lag-entrainment effects should also be included ($FFLAG = 1.0$). A lower value of $RELI$ should be used at this point ($RELI \approx 0.5$).

The third inviscid calculation is then performed. To include all the viscous effects from the second boundary-layer calculation, $BLCP$ should be set equal to 2.0. Since the viscous corrections applied for the third inviscid calculation should be about the same as the corrections applied for the second inviscid calculation, the inviscid flow field will not be very different. Hence, the third inviscid calculation should start with the values of the potential left from the end of the second inviscid calculation. The third boundary-layer calculation is then performed. $RELI$ should be equal to approximately 0.5.

The fourth and ensuing calculations of the inviscid flow field and boundary layer use the same input parameters. All inviscid calculations are performed

on the fine grid, and each inviscid calculation starts with the solution from the previous calculation. Typically, 20 cycles should be performed in each inviscid calculation. Full boundary-layer treatment ($BLCP = 2.0$) and lag-entrainment effects ($FFLAG = 1.0$) should be included and their changes underrelaxed ($RELI = 0.5$). Realistic transition points for the upper- and lower-surface boundary layers should be used. The blocks of inviscid and viscous calculations should continue until convergence is obtained. Normally, this takes 5-8 global iterations.

There are several criteria to consider when deciding if a run is properly converged. A rough measure of the convergence is the configuration lift coefficient, which may be used if the user is interested only in the overall lift. A better measure of convergence is the lift distribution in the inviscid calculation. As with the total lift, changes in the lift distribution should be observed over several global iterations to determine convergence. The number of sonic points in the inviscid flow field should also be used as a measure of convergence for calculations of transonic flow. If a run is determined to be insufficiently converged, the restart option should be used to continue the calculation.

The aforementioned running strategies are not hard and fast rules. For difficult cases, it may be necessary to change some of the relaxation parameters (reduce $P10$, $P20$, $P30$, $RELI$, QC , and/or increase $FIT10$ and $FIT20$). For very difficult cases, it may help to bring in the viscous corrections more slowly rather than having them all in place by the third global iteration. Constant-value extrapolation of the displacement thickness through regions of separation ($FISEPI(1) = 0.0$ and $FISEPI(2) = 0.0$) for the first few boundary-layer calculations may be helpful. This is especially true in the cove region of a wing with a supercritical airfoil section. Purely turbulent boundary-layer calculations ($AK(1) = AK(2) = 0.0$) for the first few boundary-layer calculations will not only speed convergence but may actually help convergence of solutions for difficult cases.

The sharpness of shocks is affected by the artificial viscosity used as damping in the inviscid calculation. There are two input parameters related to the artificial viscosity, VIS and QC . VIS switches the artificial viscosity from first to second order, with the second-order artificial viscosity giving sharper shocks. QC is the square of the Mach number above which the viscosity is applied. QC may be increased in final global iterations to as high as 0.99, but lower values (0.96 to 0.98) are usually required in the early stages of the calculation to provide additional damping and to speed convergence.

Output Description

This section of the report is intended to outline the output of TAWFIVE (output to unit 6). This outline helps explain the output to the new user but does not cover the subject in complete detail.

The first page of the output is simply a header identifying TAWFIVE. Next follows an echo of the inviscid-iteration and global-iteration control input data from unit 5. The next page starts with the run title from read order 1 from unit 5. A message that the program "READ FROM RESTART TAPE" is next, if applicable.

A summary of the input geometry is then given, and the length of the summary is controlled by FPLOTT. In the grid generation, a parabola is curve fitted to the leading edge of the input stations. If this curve fit is not sufficiently accurate, a warning message is issued and the deviation of the leading-edge point from the parabola is printed. This deviation is DXAM; large values indicate improper geometric definitions of the respective section, and thus corrections are necessary. If insufficient definition of the leading edge is provided, a warning message is given that fewer than five points are forward of the calculated singular point. Basic and modified trailing-edge slopes and the included angles are also given. The modified values reflect changes due to the boundary-layer correction.

After the summary of the input geometry, some information about the grid may be displayed. It is important that the upstream extent of the grid off the wingtip lies ahead of the wing-root leading edge for proper alignment of the domains of dependence. This can be confirmed by checking to see that the numerical value of the last point of the first grid line in the printout (x -coordinate of the wing-root leading edge) is greater than the numerical value of the first point of the second grid line in the printout (x -coordinate of the upstream limit of the grid off the wingtip). If the grid has too much sweep, a warning is given. The position of the point off the tip can be changed by adjusting SWEEP.

The next part of the printout contains the inviscid-iteration listing for the present global iteration. Some of the input is echoed and then iteration statistics follow. Column 1 is the multigrid cycle, and column 2 indicates whether XSWEEP(1) or YSWEEP(0) is being used on the fine grid. Column 3 shows the value of the maximum change made to the potential function at the point indicated in columns 4-6. Column 7 gives the average of the absolute value of the correction made to the potential function over all points in the grid. Column 8 indicates the maximum residual that is located at the

point in the flow field indicated in columns 9-11. Column 12 displays the average of the absolute values of the residual over all points in the flow field.

Column 13 shows the value of the circulation at the root. Numerically, this is the jump in potential at the trailing edge at the root. Physically, it is proportional to the root-section lift coefficient.

Column 14 gives cumulative work for the current global iteration. (One unit of work is equivalent to one fine-grid iteration.) Column 15 shows the number of supersonic points in the flow field.

The last two columns, 16 and 17, present the current wing lift coefficient and angle of attack. The lift coefficient is based on the circulation at each of the airfoil sections (eq. (7)), not on an integration of pressures on the wing. It is this lift that is matched to the prescribed lift coefficient (CLSPEC) if FCL = 1.0. The angle of attack is the input angle if the code is used in the angle-of-attack prescribed mode (FCL = 0.0). Otherwise, the value is the current iterated angle of attack adjusted to match the prescribed lift coefficient (FCL = 1.0). Some residual history-summary data, as well as CPU time for the current iterations, are listed after the iteration history. Wing-section data are then presented. If FPLOTT \geq 2, printer C_p plots are written for each of the computational stations. For FPLOTT < 2, only a summary of the section lift, drag, and pitching-moment coefficients is displayed. These values are based on integrated pressures. A table of the wing and fuselage coefficients is then given.

The next page of the output shows the calculated boundary-layer starting data. The boundary-layer calculation for each surface is begun just aft of the leading edge at a chord fraction located somewhere between XPROZF and XPROZR. The spanwise-constant starting point is determined in the boundary-layer starting routine. Calculated forward and rearward limits for the boundary-layer starting point for the upper and lower surfaces for each section are first indicated. Then, the calculated brackets for the wing are given. These values replace XPROZF and XPROZR if XPROZR(1) or XPROZR(2) is input as zero. (See table 4.)

The next page begins the boundary-layer output portion of the printout. The first page is an echo of some of the input data. The following description of the rest of the boundary-layer printout is for FFIPRN = -1.0. The printout generated beyond this option is self-explanatory.

Boundary-layer data for the upper surface are presented first; these data cover the leading edge to the trailing edge at constant chord fractions out the wing. In the blocks of printout at each chord fraction, the data are given from the root to the tip.

The columns in the blocks of data are described as follows:

- station - Span location, where 1 is the wing root and 25 is the wingtip. These sections coincide with the inviscid computational span stations.
- Z - Physical location of the span station, referenced to the geometric input coordinate system
- TE - Momentum thickness θ_{11} defined as $\int_0^\infty \frac{\rho}{\rho_e} \frac{u}{u_e} \left(1 - \frac{u}{u_e}\right) dy$, where ρ is the density, u is the velocity parallel to the wall, and the subscript e denotes a value at the edge of the boundary layer
- DELST - True three-dimensional displacement thickness (see ref. 16), δ^*
- DELSTX - Change in DELST in chord direction: $\frac{\partial}{\partial x}$ (DELST)
- CF - Magnitude of skin friction
- BETA - Wall shear angle. This is the angle between the wall shear and the external (to the boundary layer) flow directions. Positive values indicate that the shear direction is more toward the tip than the external flow.
- H,HINC - Boundary-layer shape factors (see ref. 16)
- UE - External flow speed (speed at the edge of the boundary layer), u_e
- AL - Angle between the external flow (of the boundary layer) and the x -direction. Positive values indicate flow toward the wingtip.

This block of data is repeated for several chord fractions on the upper surface (spacing controlled by XDRUCK) and is followed by blocks of output for the lower surface. The number of integration steps for each of the surfaces is output; values of 50 to 200 are normal. Very high numbers (>400) indicate problems with the boundary-layer calculation, usually separation.

Depending on the value of FFIPRN, short maps of δ^* on the upper and lower wing surfaces and upper and lower wake surfaces are printed. All these maps follow the same format. The first number in the first line is an echo of the input variable RELI. The rest

of the numbers in the first line are the span fraction, root (0.0) to tip (1.0). The rest of the lines in the maps give the chord fraction in the first column and then the values of δ^* at successive spanwise locations.

NASA Langley Research Center
Hampton, VA 23665-5225
March 20, 1989

References

1. Murman, Earll M.; and Cole, Julian D.: Calculation of Plane Steady Transonic Flows. *AIAA J.*, vol. 9, no. 1, Jan. 1971, pp. 114-121.
2. Jameson, Antony: Iterative Solution of Transonic Flows Over Airfoils and Wings, Including Flows at Mach 1. *Commun. Pure & Appl. Math.*, vol. XXVII, no. 3, May 1974, pp. 283-309.
3. Melson, N. Duane; and Streett, Craig L.: *TAWFIVE: A Users' Guide*. NASA TM-84619, 1983.
4. Vatsa, V. N.: Accurate Numerical Solutions for Transonic Viscous Flow Over Finite Wings. *J. Aircr.*, vol. 24, no. 6, June 1987, pp. 377-385.
5. Thomas, J. L.; Taylor, S. L.; and Anderson, W. K.: Navier-Stokes Computations of Vortical Flows Over Low Aspect Ratio Wings. AIAA-87-0207, Jan. 1987.
6. Fujii, Kozo; and Obayashi, Shigeru: Navier-Stokes Simulation of Transonic Flows Over Wing-Fuselage Combinations. AIAA-86-1831, June 1986.
7. Holst, Terry L.; Kaynak, Unver; Gundy, Karen L.; Thomas, Scott D.; Flores, Jolen; and Chaderjian, Neal M.: Numerical Solution of Transonic Wing Flows Using an Euler/Navier-Stokes Zonal Approach. AIAA-85-1640, July 1985.
8. Jameson, Antony; and Baker, Timothy J.: Solution of the Euler Equations for Complex Configurations. *A Collection of Technical Papers—AIAA 6th Computational Fluid Dynamics Conference, July 1983*, pp. 293-302. (Available as AIAA-83-1929.)
9. Bradshaw, P., ed.: *Turbulence, Second Corrected and Updated ed.* Springer-Verlag, 1978.
10. Caughey, D. A.: Multi-Grid Calculation of Three-Dimensional Transonic Potential Flows. *Appl. Math. & Comput.*, vol. 13, nos. 3 and 4, 1983, pp. 241-260.
11. Melson, Norman Duane: Vectorizable Multigrid Algorithms for Transonic Flow Calculations. M.S. Thesis, George Washington Univ., 1979. (Available as NASA CR-174326.)
12. Melnik, R. E.; Chow, R.; and Mead, H. R.: Theory of Viscous Transonic Flow Over Airfoils at High Reynolds Number. AIAA Paper No. 77-680, June 1977.
13. Streett, Craig L.: *Viscous-Inviscid Interaction Method Including Wake Effects for Three-Dimensional Wing-Body Configurations*. NASA TP-1910, 1981.
14. Streett, Craig L.: *Viscous-Inviscid Interaction for Transonic Wing-Body Configurations Including Wake Effects*. AIAA-81-1266, June 1981.

15. Streett, Craig L.: Viscous-Inviscid Interaction for Transonic Wing-Body Configurations Including Wake Effects. *AIAA J.*, vol. 20, no. 7, July 1982, pp. 915-923.
16. Smith, P. D.: *An Integral Prediction Method for Three-Dimensional Compressible Turbulent Boundary Layers*. R. & M. No. 3739, British Aeronautical Research Council, 1974.
17. Stock, H. W.: *Integral Method for the Calculation of Three-Dimensional, Laminar and Turbulent Boundary Layers*. NASA TM-75320, 1978.
18. Green, J. E.; Weeks, D. J.; and Brooman, J. W. F.: *Prediction of Turbulent Boundary Layers and Wakes in Compressible Flow by a Lag-Entrainment Method*. R. & M. No. 3791, British Aeronautical Research Council, 1977.
19. Young, Clarence P., Jr.: Pathfinder Model Program for the National Transonic Facility. *High Reynolds Number Research—1980*, L. Wayne McKinney and Donald D. Baals, eds., NASA CP-2183, 1981, pp. 37-52.
20. Jameson, Antony; Caughey, David A.; Newman, Perry A.; and Davis, Ruby M.: *A Brief Description of the Jameson-Caughey NYU Transonic Swept-Wing Computer Program—FLO 22*. NASA TM X-73996, 1976.

Table 1. I/O Units

<u>Unit</u>	<u>Description</u>
1	FORMATTED OUTPUT - This file contains plotting data for use by postprocessor plotting packages. It includes data for pressure coefficient C_p versus chord section; carpet plots; and residual, lift, and sonic-point iteration history plots.
3	UNFORMATTED OUTPUT - This file contains restart information. It is written by subroutine SAVE which is called by the main program INTRACT.
4	UNFORMATTED INPUT - This file contains restart information. It is read by subroutine RESTRT which is called by subroutine FLO30M.
5	FORMATTED INPUT - This file contains iteration and interaction control input variables. See table 4 for a detailed description of the input on this unit. This information is read from subroutine FLO30M which is called by the main program INTRACT.
6	FORMATTED OUTPUT - This file contains the output from the program. Included are grid information; inviscid iteration histories; and wing-section aerodynamic, configuration aerodynamic, wing boundary-layer, and wake-calculation data.
7	FORMATTED INPUT - This file contains the geometry definition input, including both body-section and wing-section definitions. These data are read in subroutine GEOM that is called by subroutine FLO30M which is called from the main program INTRACT. See table 2 for a detailed description of the input on this unit.

Table 2. Geometry Input Description for Unit 7

Read orders 1-13 are used to specify the wing geometry, and read orders 14-19 are used to define the fuselage. The wing can be defined with up to 21 span stations. A set of airfoil coordinates must be read in at the first (root) section. It need not be read in at other stations if one is changing only combinations of the following three airfoil-section parameters: chord, thickness ratio, or angle of attack (twist). The wing shapes at computational span locations between the input span locations are obtained by linear interpolations in the spanwise direction in physical space.

Read orders 1-3 are read only once.

<u>Read order</u>	<u>Number of records</u>	<u>Description and comments</u>
1	1	TITLE. - Title of geometric configuration. This title is written on unit 6 with the geometric information at the beginning of the inviscid calculation. FORMAT (20A4)
2	1	DESC. - Description for record in read order 3.
3	1	FNC, SWEEP1, SWEEP2, SWEEP, DIHED1, DIHED2, DIHED FORMAT (8F10.6) FNC. - Number of input wing sections used to define the wing geometry. A maximum of 21 and a minimum of 2 are allowed. SWEEP1. - Sweep angle of wing leading edge at root section (in degrees) as shown in figure 3. (Not used.) SWEEP2. - Sweep angle of wing leading edge at tip section (in degrees) as shown in figure 3. SWEEP. - Sweep angle of spanwise grid lines at farfield boundary (off tip of wing) (in degrees) as shown in figure 3. DIHED1. - Dihedral angle of wing leading edge at root section (in degrees) as shown in figure 4. (Not used.) DIHED2. - Dihedral angle of spanwise grid lines at tip section (off tip of wing) (in degrees) as shown in figure 4. DIHED. - Dihedral angle of wing leading edge at farfield boundary (in degrees) as shown in figure 4.

Read orders 4-10 and 12 are read once for each of the FNC wing input sections. Read orders 11 and 13 are read FNUI and FNUL times, respectively, for each of the FNC airfoil wing sections.

Table 2. Continued

<u>Read order</u>	<u>Number of records</u>	<u>Description and comments</u>
4	1	DESC. - Description for card in read order 5.
5	1	ZIN, XLIN, YLIN, CHIN, TH, ALIN, FSEC, FINT FORMAT (8F10.6)
		ZIN. - Spanwise coordinate of the wing section being specified. It is in the same units as CHIN, the input chord length for each section. The wing sections must be input starting with the wing root and continuing to the tip-section definition. The root section should be just outside the wing-fuselage intersection. See figure 5.
		XLIN. - x -coordinate of section leading edge in physical space (controls sweep). See figure 5.
		YLIN. - y -coordinate of section leading edge in physical space (controls dihedral). See figure 5.
		CHIN. - Section chord length. The chord of the airfoil coordinates to be read in (or already read in at a prior section if FSEC = 0) will be scaled to this value.
		TH. - Section thickness ratio relative to that of the airfoil coordinates to be read in (or already read in at a prior section if FSEC = 0). The thickness of the airfoil coordinates will be scaled with this value.
		ALIN. - Section angle of attack or twist (in degrees). Airfoil coordinates will be rotated through this angle about the origin of the parabolic mapping (not the airfoil leading edge).
		FSEC. - Airfoil-section-coordinate input trigger.
		FSEC = 0. Airfoil coordinates are not read in at this station; the last set of airfoil coordinates read in will be used at this station. The previous coordinates are scaled using CHIN, TH, and ALIN. Read orders 6-13 are not used for FSEC = 0.
		FSEC = 1. A new set of airfoil coordinates will be read in at this station.

Table 2. Continued

<u>Read order</u>	<u>Number of records</u>	<u>Description and comments</u>
		FINT. - Hard-surface lofting control parameter. Boundary-layer corrections are added to a hard surface generated internally by the program by linear lofting between the input airfoil sections. FINT gives the number of equally spaced sections added between this input section and the next. $FINT \geq 0$. (FNC plus the number of sections added using FINT must be less than 21.)
6	1	DESC. - Description for record in read order 7.
7	1	YSYM, FNUI, FNLI YSYM. - Airfoil symmetry trigger. YSYM > 0. Symmetric airfoil. Read in only upper-surface airfoil coordinates, ordered leading edge to trailing edge. YSYM ≤ 0. Nonsymmetric airfoil. Read in upper- and lower-surface airfoil coordinates, respectively, each set ordered leading edge to trailing edge. Note that leading-edge point is included in both the upper- and lower-surface coordinate sets. FNUI. - Number of coordinates read in for upper surface of airfoil. ($FNUI \leq 81$.) (FNUI must be the same for all input stations.) FNLI. - Number of coordinates read in for definition of lower surface of airfoil ($FNLI \leq 81$.) (FNLI must be the same for all input stations.)
8	1	DESC. - Description for card in read order 9.
9	1	TRL, SLT, XSING, YSING FORMAT (8F10.6)

These values are not used by the program. Their values are generated internally. Read orders 8 and 9 were left in only to make the geometry input compatible with earlier versions of FLO30. For completeness and to assist readers who may use this write-up to help run FLO30, these four variables are defined below.

Table 2. Continued

<u>Read order</u>	<u>Number of records</u>	<u>Description and comments</u>
		<p>TRL. - Included angle of trailing edge of airfoil (in degrees). For blunt trailing edges, it is the upper-surface slope angle minus the lower-surface slope angle. (Not used in present work.)</p> <p>SLT. - Slope of airfoil mean camber line at trailing edge. (Not used in present work.)</p> <p>XSING. - x-coordinate of the origin of the parabolic mapping referenced to the airfoil leading edge. The recommended value is approximately $X(LE) + 1/2$ leading-edge radius where the leading-edge radius is in the same units as $XP(I)$ read in below. (Not used in present work.)</p> <p>YSING. - y-coordinate of the origin of the mapping referenced to the airfoil leading edge. The recommended value is approximately $Y(LE)$. (Not used in present work.)</p>
10	1	DESC. - Description for records in read order 11.
11	FNUI	<p>XP(I), YP(I) FORMAT (8F10.6)</p> <p>XP(I). - x-coordinate of airfoil upper surface, ordered leading edge to trailing edge.</p> <p>YP(I). - y-coordinate of airfoil upper surface, ordered leading edge to trailing edge. Note that there is only one pair of coordinates per record.</p>
<p>If the airfoil section is not symmetric ($YSYM \geq 0$), the airfoil lower-surface coordinates must be read here. For a symmetric airfoil ($YSYM > 0$), skip the two read orders 12 and 13.</p>		
12	1	DESC. - Description for records in read order 13. FORMAT (8A10)
13	FNLI	<p>XP(I), YP(I) FORMAT (8F10.6)</p> <p>XP(I). - x-coordinate of airfoil lower surface, ordered leading edge to trailing edge.</p> <p>YP(I). - y-coordinate of airfoil lower surface, ordered leading edge to trailing edge. Note that there is only one pair of coordinates per record.</p>

Read orders 4-13 complete the input for one span station. As indicated above read order 4, at least read orders 4 and 5 must be repeated for the remaining FNC-1 sections where $FNC \geq 2$.

Table 2. Continued

<u>Read order</u>	<u>Number of records</u>	<u>Description and comments</u>
Read orders 14-19 are used to define the fuselage.		
14	1	DESC. - Description for record in read order 15.
15	1	FNF, FCIRC FORMAT (8F10.6)
		FNF. - Number of fuselage-defining stations. The stations are input starting at the upstream end and continuing to the downstream end of the fuselage. A maximum of 25 stations may be input.
		FCIRC. - Circular fuselage trigger.
		FCIRC = 0. Arbitrary fuselage shape is read in read orders 16-19.
		FCIRC \neq 0. Circular fuselage is used. The diameter is specified by inputting the points of intersection between the fuselage section and the $z = 0$ symmetry plane.
The block of read orders 16-19 is repeated for each of the fuselage sections used to define the fuselage.		
16	1	DESC. - Description for record in read order 17.
17	1	FNFP, XF(I), FSEC FORMAT (8F10.6)
		FNFP. - Number of coordinate pairs read in to define fuselage section ($1 \leq \text{FNFP} \leq 101$).
		FNFP = 1. This value is used to define either the nose or tail of a closed fuselage.
		FNFP = 2. This value is used with FSEC = 0. to allow scaling of previously input fuselage section.
		This value also may be used at the last fuselage station. With this, the fuselage is continued downstream as a constant area sting.

Table 2. Concluded

<u>Read order</u>	<u>Number of records</u>	<u>Description and comments</u>
		<p>This may also be used with FCIRC = 1. to input a circular fuselage. The two points input are then the intersection points of the fuselage section with the $z = 0$ symmetry plane.</p> <p>FNFP = 3. → 101. This is simply the number of coordinate pairs used to define the fuselage section.</p> <p>XF(I). - x-coordinate of the fuselage section being specified. It is in the same units as those of the wing-section chord lengths (CHIN).</p> <p>FSEC. - Fuselage-section-coordinate input trigger.</p> <p>FSEC = 0. Fuselage coordinates are not input at this station; the last set of fuselage-section coordinates read in will be scaled and used at this station. To input scaling, set FNFP = 2. to input only two points and then input the two points of intersection of the fuselage section and the $z = 0$ symmetry plane.</p> <p>FSEC = 1. A new set of fuselage-section coordinates will be read in using read orders 18 and 19.</p>
18	1	DESC. - Description for record(s) in read order 19.
19	FNFP	<p>YF, ZF FORMAT (8F10.6)</p> <p>YF. - y-coordinate of fuselage surface, ordered top of fuselage (at $z = 0$ symmetry plane) to bottom of fuselage (at $z = 0$ symmetry plane).</p> <p>ZF. - z-coordinate of fuselage surface, ordered top of fuselage (at $z = 0$ symmetry plane) to bottom of fuselage (at $z = 0$ symmetry plane).</p>

Table 3. Sample Input File of Geometric Data for Unit 7

```

pathfinder 1 nominal coordinates lh wing
fnc sweep1 sweep2 sweep dihedral1 dihedral2 dihedral
19.00000 37.12370 30.02712 30.02712 5.00000 5.00000 5.00000
xlin xlin ylin chin th alin fsec fint
2.88000 2.18000 0.00000 11.40000 1.00000 0.00000 1.00000 0.00000
ysym fnui fnli
0.00000 60.00000 60.00000
trl slit xsing ysing
0.00000 0.00000 0.00000 0.00000
upper surface
0.00000 0.00000
.00200 .01006
.00500 .01542
.01000 .02076
.02000 .02835
.03000 .03383
.04000 .03784
.05000 .04135
.06000 .04456
.07000 .04741
.08000 .04992
.09000 .05211
.10000 .05401
.11000 .05569
.12000 .05718
.13000 .05850
.14000 .05972
.15000 .06079
.16000 .06166
.17000 .06250
.18000 .06319
.19000 .06379
.20000 .06433
.22000 .06501
.24000 .06540
.26000 .06551
.28000 .06526
.30000 .06470
.32000 .06383
.34000 .06269
.36000 .06127
.38000 .05963
.42000 .05577
.46000 .05135
.50000 .04656
.52000 .04407
.54000 .04154
.56000 .03900
.58000 .03645
.60000 .03388
.62000 .03131
.64000 .02876
.66000 .02623
.68000 .02370
.70000 .02117
.72000 .01864
.74000 .01610
.76000 .01352
.78000 .01090
.80000 .00822
.82000 .00550
.84000 .00273
.86000 -.00008
.88000 -.00296
.90000 -.00590
.92000 -.00890
.94000 -.01196
.96000 -.01510
.98000 -.01828
1.00000 -.02152
lower surface
0.00000 0.00000
.00200 -.00683
.00500 -.01339
.01000 -.02004
.02000 -.02779
.03000 -.03292
.04000 -.03690
.05000 -.04020
.06000 -.04318
.07000 -.04599
.08000 -.04867
.09000 -.05118
.10000 -.05354
.11000 -.05577
.12000 -.05789
.13000 -.05992
.14000 -.06186

```

ORIGINAL PAGE IS
OF POOR QUALITY

Table 3. Continued

.15000 -.06374
 .16000 -.06551
 .17000 -.06717
 .18000 -.06875
 .19000 -.07027
 .20000 -.07162
 .22000 -.07408
 .24000 -.07621
 .26000 -.07804
 .28000 -.07959
 .30000 -.08084
 .32000 -.08191
 .34000 -.08271
 .36000 -.08318
 .38000 -.08349
 .42000 -.08328
 .46000 -.08203
 .50000 -.07990
 .52000 -.07853
 .54000 -.07692
 .56000 -.07504
 .58000 -.07294
 .60000 -.07062
 .62000 -.06814
 .64000 -.06541
 .66000 -.06240
 .68000 -.05922
 .70000 -.05580
 .72000 -.05226
 .74000 -.04858
 .76000 -.04485
 .78000 -.04109
 .80000 -.03747
 .82000 -.03408
 .84000 -.03099
 .86000 -.02823
 .88000 -.02604
 .90000 -.02442
 .92000 -.02351
 .94000 -.02327
 .96000 -.02378
 .98000 -.02525
 1.00000 -.02778
 zlin xlin ylin chin th alin fsec fcut
 3.49000 2.66000 0.00000 10.92000 1.00000 0.00000 1.00000 0.00000
 ysym fnul fnli
 0.00000 60.00000 60.00000
 trl slt xsing ysing
 0.00000 0.00000 0.00000 0.00000
 upper surface
 0.00000 0.00000
 .00200 .00971
 .00500 .01525
 .01000 .02075
 .02000 .02830
 .03000 .03358
 .04000 .03747
 .05000 .04085
 .06000 .04391
 .07000 .04664
 .08000 .04906
 .09000 .05118
 .10000 .05304
 .11000 .05469
 .12000 .05615
 .13000 .05746
 .14000 .05865
 .15000 .05969
 .16000 .06056
 .17000 .06139
 .18000 .06206
 .19000 .06265
 .20000 .06317
 .22000 .06387
 .24000 .06429
 .26000 .06442
 .28000 .06423
 .30000 .06375
 .32000 .06299
 .34000 .06199
 .36000 .06073
 .38000 .05926
 .42000 .05579
 .46000 .05178
 .50000 .04741
 .52000 .04513
 .54000 .04279
 .56000 .04041

ORIGINAL PAGE IS
 OF POOR QUALITY

Table 3. Continued

.58000	.03801
.60000	.03557
.62000	.03310
.64000	.03063
.66000	.02816
.68000	.02568
.70000	.02318
.72000	.02065
.74000	.01810
.76000	.01550
.78000	.01286
.80000	.01016
.82000	.00740
.84000	.00459
.86000	.00172
.88000	-.00120
.90000	-.00419
.92000	-.00725
.94000	-.01038
.96000	-.01360
.98000	-.01687
1.00000	-.02019
lower surface	
0.00000	0.00000
.00200	-.00799
.00500	-.01414
.01000	-.02050
.02000	-.02800
.03000	-.03298
.04000	-.03687
.05000	-.04012
.06000	-.04305
.07000	-.04581
.08000	-.04845
.09000	-.05093
.10000	-.05325
.11000	-.05544
.12000	-.05751
.13000	-.05949
.14000	-.06137
.15000	-.06319
.16000	-.06490
.17000	-.06650
.18000	-.06802
.19000	-.06945
.20000	-.07076
.22000	-.07312
.24000	-.07512
.26000	-.07683
.28000	-.07827
.30000	-.07939
.32000	-.08031
.34000	-.08095
.36000	-.08128
.38000	-.08141
.42000	-.08092
.46000	-.07948
.50000	-.07721
.52000	-.07578
.54000	-.07411
.56000	-.07219
.58000	-.07005
.60000	-.06769
.62000	-.06516
.64000	-.06239
.66000	-.05938
.68000	-.05620
.70000	-.05282
.72000	-.04931
.74000	-.04568
.76000	-.04201
.78000	-.03833
.80000	-.03478
.82000	-.03145
.84000	-.02842
.86000	-.02574
.88000	-.02361
.90000	-.02208
.92000	-.02129
.94000	-.02121
.96000	-.02189
.98000	-.02353
1.00000	-.02618

ORIGINAL PAGE IS
OF POOR QUALITY

zlin	xlin	ylin	chin	th	alin	fsec	fint
3.98000	3.04000	0.000000	10.54000	1.00000	0.00000	1.00000	0.00000
ysym	fnui	fnli					
0.00000	60.00000	60.00000					
trl	slt	xsing	ysing				

Table 3. Continued

ORIGINAL PAGE IS
OF POOR QUALITY

0.00000	0.00000	0.00000	0.00000
upper surface			
0.00000	0.00000		
.00200	.00940		
.00500	.01509		
.01000	.02073		
.02000	.02825		
.03000	.03336		
.04000	.03715		
.05000	.04041		
.06000	.04335		
.07000	.04598		
.08000	.04831		
.09000	.05036		
.10000	.05219		
.11000	.05381		
.12000	.05526		
.13000	.05656		
.14000	.05771		
.15000	.05873		
.16000	.05961		
.17000	.06041		
.18000	.06108		
.19000	.06166		
.20000	.06217		
.22000	.06287		
.24000	.06331		
.26000	.06347		
.28000	.06333		
.30000	.06292		
.32000	.06226		
.34000	.06136		
.36000	.06025		
.38000	.05894		
.42000	.05579		
.46000	.05215		
.50000	.04813		
.52000	.04603		
.54000	.04384		
.56000	.04162		
.58000	.03935		
.60000	.03701		
.62000	.03463		
.64000	.03223		
.66000	.02981		
.68000	.02737		
.70000	.02490		
.72000	.02238		
.74000	.01980		
.76000	.01719		
.78000	.01453		
.80000	.01181		
.82000	.00901		
.84000	.00617		
.86000	.00325		
.88000	.00028		
.90000	-.00275		
.92000	-.00586		
.94000	-.00905		
.96000	-.01233		
.98000	-.01568		
1.00000	-.01908		
lower surface			
0.00000	0.00000		
.00200	-.00896		
.00500	-.01481		
.01000	-.02090		
.02000	-.02819		
.03000	-.03304		
.04000	-.03684		
.05000	-.04005		
.06000	-.04293		
.07000	-.04566		
.08000	-.04827		
.09000	-.05071		
.10000	-.05301		
.11000	-.05515		
.12000	-.05719		
.13000	-.05911		
.14000	-.06095		
.15000	-.06271		
.16000	-.06438		
.17000	-.06593		
.18000	-.06739		
.19000	-.06876		
.20000	-.07002		
.22000	-.07230		
.24000	-.07418		

Table 3. Continued

.26000	-.07579						
.28000	-.07713						
.30000	-.07815						
.32000	-.07893						
.34000	-.07944						
.36000	-.07965						
.38000	-.07963						
.42000	-.07890						
.46000	-.07730						
.50000	-.07490						
.52000	-.07341						
.54000	-.07169						
.56000	-.06974						
.58000	-.06756						
.60000	-.06517						
.62000	-.06260						
.64000	-.05980						
.66000	-.05679						
.68000	-.05362						
.70000	-.05026						
.72000	-.04679						
.74000	-.04320						
.76000	-.03958						
.78000	-.03596						
.80000	-.03247						
.82000	-.02920						
.84000	-.02622						
.86000	-.02362						
.88000	-.02154						
.90000	-.02008						
.92000	-.01940						
.94000	-.01947						
.96000	-.02030						
.98000	-.02207						
1.00000	-.02484						
	zlin	ylin	chin	th	alin	fsec	fint
4.98000	3.79000	0.00000	9.79000	1.00000	0.00000	1.00000	0.00000
	ysym	fnui	fnli				
0.00000	60.00000	60.00000					
	trl	slt	xsing	ysing			
0.00000	0.00000	0.00000	0.00000	0.00000			
	upper surface						
0.00000	0.00000						
.00200	.00872						
.00500	.01476						
.01000	.02072						
.02000	.02814						
.03000	.03288						
.04000	.03644						
.05000	.03946						
.06000	.04211						
.07000	.04452						
.08000	.04666						
.09000	.04858						
.10000	.05035						
.11000	.05190						
.12000	.05331						
.13000	.05457						
.14000	.05567						
.15000	.05663						
.16000	.05750						
.17000	.05827						
.18000	.05892						
.19000	.05948						
.20000	.05995						
.22000	.06069						
.24000	.06118						
.26000	.06138						
.28000	.06137						
.30000	.06111						
.32000	.06067						
.34000	.06004						
.36000	.05922						
.38000	.05826						
.42000	.05583						
.46000	.05298						
.50000	.04975						
.52000	.04803						
.54000	.04621						
.56000	.04430						
.58000	.04231						
.60000	.04021						
.62000	.03804						
.64000	.03577						
.66000	.03348						
.68000	.03112						
.70000	.02871						
.72000	.02620						

ORIGINAL PAGE IS
OF POOR QUALITY

Table 3. Continued

ORIGINAL PAGE IS
OF POOR QUALITY

.74000	.02361							
.76000	.02097							
.78000	.01827							
.80000	.01548							
.82000	.01261							
.84000	.00967							
.86000	.00666							
.88000	.00359							
.90000	.00048							
.92000	-.00276							
.94000	-.00609							
.96000	-.00950							
.98000	-.01302							
1.00000	-.01660							
	lower surface							
0.00000	0.00000							
.00200	-.01112							
.00500	-.01630							
.01000	-.02181							
.02000	-.02860							
.03000	-.03317							
.04000	-.03679							
.05000	-.03988							
.06000	-.04269							
.07000	-.04533							
.08000	-.04784							
.09000	-.05025							
.10000	-.05246							
.11000	-.05451							
.12000	-.05646							
.13000	-.05831							
.14000	-.06003							
.15000	-.06166							
.16000	-.06321							
.17000	-.06466							
.18000	-.06599							
.19000	-.06721							
.20000	-.06837							
.22000	-.07046							
.24000	-.07210							
.26000	-.07348							
.28000	-.07461							
.30000	-.07538							
.32000	-.07586							
.34000	-.07607							
.36000	-.07602							
.38000	-.07564							
.42000	-.07438							
.46000	-.07242							
.50000	-.06975							
.52000	-.06815							
.54000	-.06632							
.56000	-.06428							
.58000	-.06201							
.60000	-.05956							
.62000	-.05689							
.64000	-.05404							
.66000	-.05101							
.68000	-.04785							
.70000	-.04456							
.72000	-.04117							
.74000	-.03768							
.76000	-.03417							
.78000	-.03070							
.80000	-.02735							
.82000	-.02420							
.84000	-.02134							
.86000	-.01888							
.88000	-.01692							
.90000	-.01565							
.92000	-.01519							
.94000	-.01557							
.96000	-.01674							
.98000	-.01883							
1.00000	-.02184							
	zlin	xlin	ylin	chin	th	alin	fsec	fint
5.98000	4.55000	0.00000		9.03000	1.00000	0.00000	1.00000	0.00000
	ysym	fnui	fnli					
0.00000	60.00000	60.00000	60.00000					
	trl	slt	xsing	ysing				
0.00000	0.00000	0.00000	0.00000	0.00000				
	upper surface							
0.00000	0.00000							
.00200	.00862							
.00500	.01443							
.01000	.02034							
.02000	.02777							
.03000	.03258							

Table 3. Continued

.04000	.03606
.05000	.03896
.06000	.04151
.07000	.04383
.08000	.04587
.09000	.04769
.10000	.04935
.11000	.05075
.12000	.05202
.13000	.05316
.14000	.05417
.15000	.05508
.16000	.05588
.17000	.05660
.18000	.05724
.19000	.05778
.20000	.05829
.22000	.05911
.24000	.05969
.26000	.06005
.28000	.06021
.30000	.06021
.32000	.06007
.34000	.05977
.36000	.05929
.38000	.05866
.42000	.05696
.46000	.05482
.50000	.05218
.52000	.05074
.54000	.04916
.56000	.04747
.58000	.04568
.60000	.04374
.62000	.04171
.64000	.03958
.66000	.03739
.68000	.03515
.70000	.03284
.72000	.03041
.74000	.02788
.76000	.02531
.78000	.02265
.80000	.01991
.82000	.01706
.84000	.01415
.86000	.01116
.88000	.00811
.90000	.00498
.92000	.00177
.94000	-.00150
.96000	-.00486
.98000	-.00832
1.00000	-.01186
lower surface	
0.00000	0.00000
.00200	-.01115
.00500	-.01622
.01000	-.02158
.02000	-.02826
.03000	-.03281
.04000	-.03639
.05000	-.03938
.06000	-.04201
.07000	-.04446
.08000	-.04678
.09000	-.04895
.10000	-.05094
.11000	-.05279
.12000	-.05452
.13000	-.05612
.14000	-.05762
.15000	-.05902
.16000	-.06032
.17000	-.06155
.18000	-.06267
.19000	-.06372
.20000	-.06470
.22000	-.06643
.24000	-.06780
.26000	-.06894
.28000	-.06982
.30000	-.07041
.32000	-.07076
.34000	-.07087
.36000	-.07075
.38000	-.07041
.42000	-.06919

ORIGINAL PAGE IS
OF POOR QUALITY

Table 3. Continued

ORIGINAL PAGE IS
OF POOR QUALITY

.46000	-.06727						
.50000	-.06456						
.52000	-.06289						
.54000	-.06095						
.56000	-.05883						
.58000	-.05643						
.60000	-.05388						
.62000	-.05111						
.64000	-.04818						
.66000	-.04507						
.68000	-.04184						
.70000	-.03844						
.72000	-.03498						
.74000	-.03148						
.76000	-.02797						
.78000	-.02455						
.80000	-.02128						
.82000	-.01827						
.84000	-.01560						
.86000	-.01335						
.88000	-.01169						
.90000	-.01068						
.92000	-.01042						
.94000	-.01093						
.96000	-.01221						
.98000	-.01432						
1.00000	-.01727						
	zlin	ylin	chin	th	alin	fsec	fint
6.72000	5.12000	0.000000	8.46000	1.00000	0.00000	1.00000	0.00000
	ysym	fnui	fnli				
0.00000	60.000000	60.000000					
	trl	slt	xsing	ysing			
0.00000	0.000000	0.000000	0.000000				
	upper surface						
0.00000	0.000000						
.00200	.00849						
.00500	.01410						
.01000	.01998						
.02000	.02744						
.03000	.03229						
.04000	.03572						
.05000	.03853						
.06000	.04100						
.07000	.04322						
.08000	.04516						
.09000	.04690						
.10000	.04847						
.11000	.04975						
.12000	.05091						
.13000	.05196						
.14000	.05290						
.15000	.05376						
.16000	.05452						
.17000	.05520						
.18000	.05582						
.19000	.05637						
.20000	.05691						
.22000	.05781						
.24000	.05846						
.26000	.05895						
.28000	.05927						
.30000	.05949						
.32000	.05961						
.34000	.05958						
.36000	.05939						
.38000	.05905						
.42000	.05795						
.46000	.05639						
.50000	.05426						
.52000	.05304						
.54000	.05168						
.56000	.05018						
.58000	.04856						
.60000	.04678						
.62000	.04486						
.64000	.04284						
.66000	.04075						
.68000	.03862						
.70000	.03639						
.72000	.03401						
.74000	.03156						
.76000	.02903						
.78000	.02642						
.80000	.02373						
.82000	.02089						
.84000	.01800						
.86000	.01503						
.88000	.01199						

Table 3. Continued

.90000	.00884						
.92000	.00566						
.94000	.00243						
.96000	-.00087						
.98000	-.00427						
1.00000	-.00778						
lower surface							
0.00000	0.00000						
.00200	-.01113						
.00500	-.01613						
.01000	-.02136						
.02000	-.02797						
.03000	-.03250						
.04000	-.03604						
.05000	-.03894						
.06000	-.04142						
.07000	-.04370						
.08000	-.04585						
.09000	-.04782						
.10000	-.04959						
.11000	-.05126						
.12000	-.05283						
.13000	-.05421						
.14000	-.05550						
.15000	-.05667						
.16000	-.05777						
.17000	-.05880						
.18000	-.05975						
.19000	-.06063						
.20000	-.06144						
.22000	-.06285						
.24000	-.06399						
.26000	-.06491						
.28000	-.06557						
.30000	-.06602						
.32000	-.06626						
.34000	-.06630						
.36000	-.06614						
.38000	-.06584						
.42000	-.06472						
.46000	-.06285						
.50000	-.06013						
.52000	-.05840						
.54000	-.05636						
.56000	-.05415						
.58000	-.05166						
.60000	-.04901						
.62000	-.04616						
.64000	-.04317						
.66000	-.03998						
.68000	-.03667						
.70000	-.03317						
.72000	-.02964						
.74000	-.02614						
.76000	-.02263						
.78000	-.01924						
.80000	-.01605						
.82000	-.01316						
.84000	-.01065						
.86000	-.00859						
.88000	-.00719						
.90000	-.00641						
.92000	-.00633						
.94000	-.00696						
.96000	-.00832						
.98000	-.01046						
1.00000	-.01334						
zlin	xlin	ylin	chin	th	alin	fsec	fint
7.47000	5.69000	0.000000	7.89000	1.00000	0.00000	1.00000	0.00000
ysym	fnui	fnli					
0.00000	60.00000	60.00000					
trl	slt	xsing	ysing				
0.00000	0.00000	0.00000	0.00000				
upper surface							
0.00000	0.00000						
.00200	.00839						
.00500	.01407						
.01000	.01989						
.02000	.02735						
.03000	.03227						
.04000	.03579						
.05000	.03861						
.06000	.04099						
.07000	.04306						
.08000	.04488						
.09000	.04652						
.10000	.04800						
.11000	.04931						

ORIGINAL PAGE IS
OF POOR QUALITY

Table 3. Continued

.12000	.05050
.13000	.05159
.14000	.05257
.15000	.05348
.16000	.05432
.17000	.05509
.18000	.05580
.19000	.05644
.20000	.05704
.22000	.05806
.24000	.05889
.26000	.05955
.28000	.06004
.30000	.06039
.32000	.06062
.34000	.06068
.36000	.06059
.38000	.06040
.42000	.05965
.46000	.05834
.50000	.05650
.52000	.05543
.54000	.05423
.56000	.05290
.58000	.05142
.60000	.04980
.62000	.04808
.64000	.04625
.66000	.04430
.68000	.04225
.70000	.04005
.72000	.03772
.74000	.03527
.76000	.03272
.78000	.03006
.80000	.02731
.82000	.02444
.84000	.02148
.86000	.01842
.88000	.01526
.90000	.01202
.92000	.00871
.94000	.00533
.96000	.00188
.98000	-.00169
1.00000	-.00537
lower surface	
0.00000	0.00000
.00200	-.01079
.00500	-.01568
.01000	-.02084
.02000	-.02739
.03000	-.03191
.04000	-.03544
.05000	-.03835
.06000	-.04084
.07000	-.04305
.08000	-.04512
.09000	-.04699
.10000	-.04869
.11000	-.05029
.12000	-.05179
.13000	-.05313
.14000	-.05437
.15000	-.05550
.16000	-.05654
.17000	-.05751
.18000	-.05838
.19000	-.05921
.20000	-.05995
.22000	-.06124
.24000	-.06225
.26000	-.06308
.28000	-.06373
.30000	-.06415
.32000	-.06440
.34000	-.06449
.36000	-.06439
.38000	-.06415
.42000	-.06313
.46000	-.06127
.50000	-.05847
.52000	-.05664
.54000	-.05451
.56000	-.05216
.58000	-.04947
.60000	-.04658
.62000	-.04348

ORIGINAL PAGE IS
OF POOR QUALITY

Table 3. Continued

.64000	-.04022							
.66000	-.03677							
.68000	-.03319							
.70000	-.02949							
.72000	-.02576							
.74000	-.02209							
.76000	-.01853							
.78000	-.01513							
.80000	-.01196							
.82000	-.00912							
.84000	-.00673							
.86000	-.00484							
.88000	-.00356							
.90000	-.00289							
.92000	-.00294							
.94000	-.00372							
.96000	-.00522							
.98000	-.00750							
1.00000	-.01056							
zlin	xlin	ylin	chin	th	alin	fsec	fint	
8.97000	6.83000	0.000000	6.83000	1.00000	0.00000	1.00000	0.00000	
ysym	fnul	fnli						
0.00000	60.00000	60.00000						
trl	slt	xsing	ysing					
0.00000	0.00000	0.00000	0.00000					
upper surface								
0.00000	0.00000							
.00200	.00832							
.00500	.01385							
.01000	.01947							
.02000	.02680							
.03000	.03179							
.04000	.03539							
.05000	.03833							
.06000	.04076							
.07000	.04285							
.08000	.04469							
.09000	.04638							
.10000	.04791							
.11000	.04930							
.12000	.05061							
.13000	.05181							
.14000	.05294							
.15000	.05399							
.16000	.05497							
.17000	.05588							
.18000	.05675							
.19000	.05756							
.20000	.05829							
.22000	.05960							
.24000	.06073							
.26000	.06170							
.28000	.06249							
.30000	.06312							
.32000	.06362							
.34000	.06393							
.36000	.06413							
.38000	.06421							
.42000	.06405							
.46000	.06330							
.50000	.06208							
.52000	.06130							
.54000	.06041							
.56000	.05938							
.58000	.05822							
.60000	.05691							
.62000	.05549							
.64000	.05398							
.66000	.05231							
.68000	.05052							
.70000	.04856							
.72000	.04646							
.74000	.04418							
.76000	.04178							
.78000	.03922							
.80000	.03654							
.82000	.03372							
.84000	.03076							
.86000	.02767							
.88000	.02440							
.90000	.02103							
.92000	.01738							
.94000	.01374							
.96000	.00995							
.98000	.00598							
1.00000	.00183							
lower surface								
0.00000	0.00000							

ORIGINAL PAGE IS
OF POOR QUALITY

Table 3. Continued

ORIGINAL PAGE IS
OF POOR QUALITY

.00200	-.00935							
.00500	-.01429							
.01000	-.01949							
.02000	-.02613							
.03000	-.03059							
.04000	-.03411							
.05000	-.03700							
.06000	-.03951							
.07000	-.04168							
.08000	-.04366							
.09000	-.04543							
.10000	-.04704							
.11000	-.04855							
.12000	-.04994							
.13000	-.05122							
.14000	-.05239							
.15000	-.05348							
.16000	-.05446							
.17000	-.05536							
.18000	-.05618							
.19000	-.05695							
.20000	-.05765							
.22000	-.05882							
.24000	-.05974							
.26000	-.06049							
.28000	-.06105							
.30000	-.06141							
.32000	-.06161							
.34000	-.06167							
.36000	-.06157							
.38000	-.06129							
.42000	-.06020							
.46000	-.05818							
.50000	-.05523							
.52000	-.05332							
.54000	-.05113							
.56000	-.04865							
.58000	-.04585							
.60000	-.04273							
.62000	-.03942							
.64000	-.03588							
.66000	-.03219							
.68000	-.02837							
.70000	-.02450							
.72000	-.02062							
.74000	-.01681							
.76000	-.01314							
.78000	-.00964							
.80000	-.00640							
.82000	-.00346							
.84000	-.00098							
.86000	.00102							
.88000	.00245							
.90000	.00330							
.92000	.00329							
.94000	.00262							
.96000	.00117							
.98000	-.00124							
1.00000	-.00457							
zlin	xlin	ychin	th	alin	fsec	fint		
9.92000	7.55000	0.000000	6.19000	1.00000	0.00000	1.00000	0.00000	
ysym	fnul	fnli						
0.00000	60.00000	60.00000						
trl	slt	xsing	ysing					
0.00000	0.00000	0.00000	0.00000					
upper surface								
0.00000	0.00000							
.00200	.00825							
.00500	.01361							
.01000	.01907							
.02000	.02624							
.03000	.03124							
.04000	.03490							
.05000	.03798							
.06000	.04050							
.07000	.04273							
.08000	.04468							
.09000	.04647							
.10000	.04812							
.11000	.04959							
.12000	.05098							
.13000	.05231							
.14000	.05353							
.15000	.05469							
.16000	.05578							
.17000	.05679							
.18000	.05776							
.19000	.05869							

Table 3. Continued

.20000	.05951
.22000	.06103
.24000	.06237
.26000	.06354
.28000	.06453
.30000	.06538
.32000	.06609
.34000	.06661
.36000	.06702
.38000	.06730
.42000	.06752
.46000	.06718
.50000	.06643
.52000	.06585
.54000	.06520
.56000	.06436
.58000	.06341
.60000	.06219
.62000	.06099
.64000	.05968
.66000	.05821
.68000	.05666
.70000	.05493
.72000	.05305
.74000	.05101
.76000	.04883
.78000	.04643
.80000	.04389
.82000	.04117
.84000	.03831
.86000	.03529
.88000	.03204
.90000	.02866
.92000	.02504
.94000	.02124
.96000	.01721
.98000	.01295
1.00000	.00843
lower surface	
0.00000	0.00000
.00200	-.00796
.00500	-.01303
.01000	-.01841
.02000	-.02515
.03000	-.02955
.04000	-.03307
.05000	-.03596
.06000	-.03846
.07000	-.04063
.08000	-.04259
.09000	-.04433
.10000	-.04591
.11000	-.04733
.12000	-.04868
.13000	-.04992
.14000	-.05105
.15000	-.05210
.16000	-.05305
.17000	-.05394
.18000	-.05475
.19000	-.05550
.20000	-.05621
.22000	-.05734
.24000	-.05827
.26000	-.05897
.28000	-.05947
.30000	-.05977
.32000	-.05990
.34000	-.05986
.36000	-.05969
.38000	-.05934
.42000	-.05806
.46000	-.05589
.50000	-.05285
.52000	-.05094
.54000	-.04878
.56000	-.04629
.58000	-.04352
.60000	-.04056
.62000	-.03719
.64000	-.03359
.66000	-.02984
.68000	-.02600
.70000	-.02210
.72000	-.01821
.74000	-.01435
.76000	-.01057
.78000	-.00697

ORIGINAL PAGE IS
OF POOR QUALITY

Table 3. Continued

ORIGINAL PAGE IS
OF POOR QUALITY

.80000	-.00357							
.82000	-.00048							
.84000	.00226							
.86000	.00453							
.88000	.00627							
.90000	.00746							
.92000	.00791							
.94000	.00747							
.96000	.00620							
.98000	.00379							
1.00000	.00034							
	zlin	xlin	ylin	chin	th	alin	fsec	fint
11.46000	8.51000	0.000000	5.72000	1.00000	0.00000	1.00000	0.00000	0.00000
	ysym	fnul	fnli					
0.00000	60.00000	60.00000						
	trl	slt	xsing	ysing				
0.00000	0.00000	0.00000	0.00000	0.00000				
	upper	surface						
0.00000	0.00000							
.00200	.00711							
.00500	.01193							
.01000	.01691							
.02000	.02376							
.03000	.02845							
.04000	.03203							
.05000	.03498							
.06000	.03746							
.07000	.03963							
.08000	.04154							
.09000	.04324							
.10000	.04482							
.11000	.04629							
.12000	.04768							
.13000	.04900							
.14000	.05023							
.15000	.05135							
.16000	.05244							
.17000	.05343							
.18000	.05438							
.19000	.05529							
.20000	.05617							
.22000	.05777							
.24000	.05919							
.26000	.06040							
.28000	.06148							
.30000	.06246							
.32000	.06326							
.34000	.06400							
.36000	.06462							
.38000	.06510							
.42000	.06578							
.46000	.06605							
.50000	.06584							
.52000	.06555							
.54000	.06521							
.56000	.06473							
.58000	.06409							
.60000	.06333							
.62000	.06243							
.64000	.06136							
.66000	.06017							
.68000	.05885							
.70000	.05741							
.72000	.05580							
.74000	.05404							
.76000	.05209							
.78000	.04993							
.80000	.04751							
.82000	.04489							
.84000	.04202							
.86000	.03894							
.88000	.03554							
.90000	.03190							
.92000	.02795							
.94000	.02366							
.96000	.01908							
.98000	.01414							
1.00000	.00885							
	lower	surface						
0.00000	0.00000							
.00200	-.01008							
.00500	-.01492							
.01000	-.01970							
.02000	-.02553							
.03000	-.02932							
.04000	-.03233							
.05000	-.03480							
.06000	-.03692							

Table 3. Continued

.07000	-.03881						
.08000	-.04051						
.09000	-.04199						
.10000	-.04326						
.11000	-.04444						
.12000	-.04553						
.13000	-.04652						
.14000	-.04744						
.15000	-.04831						
.16000	-.04910						
.17000	-.04982						
.18000	-.05044						
.19000	-.05101						
.20000	-.05157						
.22000	-.05243						
.24000	-.05314						
.26000	-.05370						
.28000	-.05413						
.30000	-.05432						
.32000	-.05440						
.34000	-.05429						
.36000	-.05399						
.38000	-.05350						
.42000	-.05208						
.46000	-.04994						
.50000	-.04698						
.52000	-.04510						
.54000	-.04285						
.56000	-.04025						
.58000	-.03730						
.60000	-.03404						
.62000	-.03059						
.64000	-.02700						
.66000	-.02332						
.68000	-.01964						
.70000	-.01595						
.72000	-.01230						
.74000	-.00878						
.76000	-.00534						
.78000	-.00201						
.80000	.00100						
.82000	.00381						
.84000	.00627						
.86000	.00836						
.88000	.00991						
.90000	.01085						
.92000	.01107						
.94000	.01045						
.96000	.00876						
.98000	.00602						
1.00000	.00187						
zlin	xlin	ylin	chin	th	alin	fsec	fint
12.96000	9.44000	0.000000	5.46000	1.00000	0.00000	1.00000	0.00000
ysym	fnli	fnli					
0.00000	60.00000	60.00000					
trl	slt	xsing	ysing				
0.00000	0.00000	0.00000	0.00000				
upper surface							
0.00000	0.00000						
.00200	.00723						
.00500	.01202						
.01000	.01697						
.02000	.02370						
.03000	.02836						
.04000	.03192						
.05000	.03484						
.06000	.03732						
.07000	.03949						
.08000	.04140						
.09000	.04310						
.10000	.04468						
.11000	.04618						
.12000	.04757						
.13000	.04890						
.14000	.05013						
.15000	.05127						
.16000	.05234						
.17000	.05336						
.18000	.05432						
.19000	.05524						
.20000	.05612						
.22000	.05774						
.24000	.05916						
.26000	.06040						
.28000	.06149						
.30000	.06246						
.32000	.06330						
.34000	.06405						

ORIGINAL PAGE IS
OF POOR QUALITY

Table 3. Continued

.36000	.06469
.38000	.06519
.42000	.06591
.46000	.06621
.50000	.06604
.52000	.06578
.54000	.06546
.56000	.06500
.58000	.06439
.60000	.06365
.62000	.06278
.64000	.06173
.66000	.06058
.68000	.05928
.70000	.05786
.72000	.05629
.74000	.05455
.76000	.05263
.78000	.05049
.80000	.04813
.82000	.04554
.84000	.04270
.86000	.03966
.88000	.03630
.90000	.03270
.92000	.02878
.94000	.02453
.96000	.01996
.98000	.01504
1.00000	.00975
lower surface	
0.00000	0.00000
.00200	-.00988
.00500	-.01471
.01000	-.01951
.02000	-.02531
.03000	-.02906
.04000	-.03205
.05000	-.03448
.06000	-.03659
.07000	-.03844
.08000	-.04010
.09000	-.04158
.10000	-.04284
.11000	-.04401
.12000	-.04508
.13000	-.04606
.14000	-.04696
.15000	-.04780
.16000	-.04860
.17000	-.04930
.18000	-.04989
.19000	-.05046
.20000	-.05100
.22000	-.05182
.24000	-.05251
.26000	-.05304
.28000	-.05343
.30000	-.05360
.32000	-.05366
.34000	-.05353
.36000	-.05322
.38000	-.05273
.42000	-.05126
.46000	-.04909
.50000	-.04609
.52000	-.04418
.54000	-.04194
.56000	-.03932
.58000	-.03638
.60000	-.03314
.62000	-.02968
.64000	-.02610
.66000	-.02245
.68000	-.01877
.70000	-.01507
.72000	-.01140
.74000	-.00788
.76000	-.00444
.78000	-.00110
.80000	.00195
.82000	.00476
.84000	.00725
.86000	.00934
.88000	.01090
.90000	.01184
.92000	.01208
.94000	.01147

ORIGINAL PAGE IS
OF POOR QUALITY

Table 3. Continued

.96000	.00977						
.98000	.00702						
1.00000	.00288						
zlin	xlin	ylin	chin	th	alin	fsec	fint
14.95000	10.68000	0.000000	5.10000	1.00000	0.00000	1.00000	0.00000
ysym	fnui	fnli					
0.00000	60.00000	60.00000					
trl	slt	xsing	ysing				
0.00000	0.00000	0.00000	0.00000				
upper surface							
0.00000	0.00000						
.00200	.00735						
.00500	.01210						
.01000	.01698						
.02000	.02364						
.03000	.02823						
.04000	.03175						
.05000	.03464						
.06000	.03711						
.07000	.03929						
.08000	.04119						
.09000	.04290						
.10000	.04450						
.11000	.04599						
.12000	.04741						
.13000	.04875						
.14000	.04998						
.15000	.05114						
.16000	.05223						
.17000	.05325						
.18000	.05424						
.19000	.05517						
.20000	.05605						
.22000	.05769						
.24000	.05916						
.26000	.06042						
.28000	.06153						
.30000	.06255						
.32000	.06342						
.34000	.06419						
.36000	.06485						
.38000	.06539						
.42000	.06618						
.46000	.06656						
.50000	.06646						
.52000	.06624						
.54000	.06595						
.56000	.06555						
.58000	.06497						
.60000	.06428						
.62000	.06344						
.64000	.06248						
.66000	.06136						
.68000	.06012						
.70000	.05873						
.72000	.05721						
.74000	.05553						
.76000	.05368						
.78000	.05158						
.80000	.04930						
.82000	.04677						
.84000	.04399						
.86000	.04101						
.88000	.03773						
.90000	.03419						
.92000	.03034						
.94000	.02616						
.96000	.02163						
.98000	.01673						
1.00000	.01146						
lower surface							
0.00000	0.00000						
.00200	-.00954						
.00500	-.01442						
.01000	-.01920						
.02000	-.02494						
.03000	-.02864						
.04000	-.03159						
.05000	-.03398						
.06000	-.03606						
.07000	-.03788						
.08000	-.03952						
.09000	-.04096						
.10000	-.04220						
.11000	-.04335						
.12000	-.04439						
.13000	-.04534						
.14000	-.04624						

ORIGINAL PAGE IS
OF POOR QUALITY

Table 3. Continued

ORIGINAL PAGE IS
OF POOR QUALITY

.15000	-.04707							
.16000	-.04783							
.17000	-.04850							
.18000	-.04908							
.19000	-.04962							
.20000	-.05012							
.22000	-.05092							
.24000	-.05154							
.26000	-.05204							
.28000	-.05238							
.30000	-.05250							
.32000	-.05252							
.34000	-.05237							
.36000	-.05202							
.38000	-.05150							
.42000	-.04997							
.46000	-.04773							
.50000	-.04464							
.52000	-.04273							
.54000	-.04044							
.56000	-.03782							
.58000	-.03490							
.60000	-.03165							
.62000	-.02821							
.64000	-.02464							
.66000	-.02097							
.68000	-.01727							
.70000	-.01357							
.72000	-.00990							
.74000	-.00634							
.76000	-.00286							
.78000	.00051							
.80000	.00359							
.82000	.00644							
.84000	.00896							
.86000	.01107							
.88000	.01267							
.90000	.01365							
.92000	.01391							
.94000	.01332							
.96000	.01164							
.98000	.00889							
1.00000	.00474							
zlin	xlin	ylin	chin	th	alin	fsec	fint	
15.95000	11.30000	0.000000	4.93000	1.00000	0.00000	1.00000	0.00000	
ysym	fnui							
0.00000	60.00000	60.00000						
trl	slt	xsing	ysing					
0.00000	0.00000	0.00000	0.00000					
upper surface								
0.00000	0.00000							
.00200	.00748							
.00500	.01215							
.01000	.01700							
.02000	.02361							
.03000	.02814							
.04000	.03164							
.05000	.03455							
.06000	.03701							
.07000	.03918							
.08000	.04108							
.09000	.04282							
.10000	.04443							
.11000	.04594							
.12000	.04734							
.13000	.04869							
.14000	.04994							
.15000	.05110							
.16000	.05221							
.17000	.05323							
.18000	.05422							
.19000	.05517							
.20000	.05606							
.22000	.05772							
.24000	.05919							
.26000	.06049							
.28000	.06164							
.30000	.06266							
.32000	.06357							
.34000	.06436							
.36000	.06504							
.38000	.06560							
.42000	.06643							
.46000	.06686							
.50000	.06684							
.52000	.06664							
.54000	.06637							
.56000	.06599							

Table 3. Continued

.58000	.06545						
.60000	.06480						
.62000	.06399						
.64000	.06305						
.66000	.06198						
.68000	.06077						
.70000	.05944						
.72000	.05794						
.74000	.05630						
.76000	.05446						
.78000	.05242						
.80000	.05017						
.82000	.04768						
.84000	.04496						
.86000	.04204						
.88000	.03878						
.90000	.03529						
.92000	.03150						
.94000	.02735						
.96000	.02286						
.98000	.01799						
1.00000	.01272						
	lower surface						
0.00000	0.00000						
.00200	-.00946						
.00500	-.01428						
.01000	-.01905						
.02000	-.02477						
.03000	-.02845						
.04000	-.03134						
.05000	-.03372						
.06000	-.03577						
.07000	-.03758						
.08000	-.03918						
.09000	-.04061						
.10000	-.04185						
.11000	-.04298						
.12000	-.04402						
.13000	-.04494						
.14000	-.04583						
.15000	-.04663						
.16000	-.04737						
.17000	-.04803						
.18000	-.04861						
.19000	-.04913						
.20000	-.04961						
.22000	-.05037						
.24000	-.05098						
.26000	-.05142						
.28000	-.05175						
.30000	-.05182						
.32000	-.05182						
.34000	-.05163						
.36000	-.05128						
.38000	-.05073						
.42000	-.04915						
.46000	-.04687						
.50000	-.04372						
.52000	-.04177						
.54000	-.03949						
.56000	-.03686						
.58000	-.03391						
.60000	-.03067						
.62000	-.02721						
.64000	-.02363						
.66000	-.01998						
.68000	-.01626						
.70000	-.01255						
.72000	-.00885						
.74000	-.00526						
.76000	-.00177						
.78000	.00162						
.80000	.00475						
.82000	.00762						
.84000	.01015						
.86000	.01230						
.88000	.01391						
.90000	.01490						
.92000	.01520						
.94000	.01462						
.96000	.01298						
.98000	.01022						
1.00000	.00609						
zlin	xlin	ylin	chin	th	alin	fsec	fint
17.95000	12.53000	0.00000	4.58000	1.00000	0.00000	1.00000	0.00000
ysym	fnul	fnli					
0.00000	60.00000	60.00000					
trl	slt	xsing	ysing				

ORIGINAL PAGE IS
OF POOR QUALITY

Table 3. Continued

0.00000	0.00000	0.00000	0.00000
upper surface			
0.00000	0.00000		
.00200	.00770		
.00500	.01232		
.01000	.01709		
.02000	.02355		
.03000	.02804		
.04000	.03150		
.05000	.03438		
.06000	.03685		
.07000	.03903		
.08000	.04097		
.09000	.04270		
.10000	.04435		
.11000	.04589		
.12000	.04733		
.13000	.04870		
.14000	.04999		
.15000	.05118		
.16000	.05230		
.17000	.05338		
.18000	.05439		
.19000	.05536		
.20000	.05630		
.22000	.05800		
.24000	.05956		
.26000	.06091		
.28000	.06212		
.30000	.06322		
.32000	.06417		
.34000	.06503		
.36000	.06579		
.38000	.06643		
.42000	.06740		
.46000	.06798		
.50000	.06810		
.52000	.06800		
.54000	.06781		
.56000	.06752		
.58000	.06707		
.60000	.06651		
.62000	.06580		
.64000	.06496		
.66000	.06398		
.68000	.06287		
.70000	.06161		
.72000	.06023		
.74000	.05868		
.76000	.05696		
.78000	.05502		
.80000	.05286		
.82000	.05050		
.84000	.04788		
.86000	.04509		
.88000	.04196		
.90000	.03859		
.92000	.03491		
.94000	.03088		
.96000	.02646		
.98000	.02165		
1.00000	.01645		
lower surface			
0.00000	0.00000		
.00200	-.00908		
.00500	-.01394		
.01000	-.01868		
.02000	-.02430		
.03000	-.02791		
.04000	-.03074		
.05000	-.03305		
.06000	-.03503		
.07000	-.03678		
.08000	-.03834		
.09000	-.03974		
.10000	-.04093		
.11000	-.04203		
.12000	-.04302		
.13000	-.04391		
.14000	-.04475		
.15000	-.04551		
.16000	-.04622		
.17000	-.04682		
.18000	-.04735		
.19000	-.04783		
.20000	-.04826		
.22000	-.04894		
.24000	-.04945		

ORIGINAL PAGE IS
OF POOR QUALITY

Table 3. Continued

.26000	-.04981						
.28000	-.05004						
.30000	-.05006						
.32000	-.04997						
.34000	-.04971						
.36000	-.04928						
.38000	-.04865						
.42000	-.04695						
.46000	-.04450						
.50000	-.04122						
.52000	-.03919						
.54000	-.03684						
.56000	-.03417						
.58000	-.03117						
.60000	-.02790						
.62000	-.02443						
.64000	-.02084						
.66000	-.01712						
.68000	-.01336						
.70000	-.00960						
.72000	-.00585						
.74000	-.00220						
.76000	.00137						
.78000	.00485						
.80000	.00804						
.82000	.01100						
.84000	.01359						
.86000	.01582						
.88000	.01750						
.90000	.01858						
.92000	.01892						
.94000	.01843						
.96000	.01682						
.98000	.01411						
1.00000	.01003						
zlin	xlin	ylin	chin	th	altn	fsec	fint
18.95000	13.15000	0.000000	4.41000	1.00000	0.00000	1.00000	0.00000
ysym	fnli	fnli					
0.00000	60.00000	60.00000					
trl	slt	xsing	ysing				
0.00000	0.00000	0.00000	0.00000				
upper surface							
0.00000	0.00000						
.00200	.00775						
.00500	.01236						
.01000	.01711						
.02000	.02350						
.03000	.02797						
.04000	.03143						
.05000	.03429						
.06000	.03676						
.07000	.03896						
.08000	.04091						
.09000	.04267						
.10000	.04432						
.11000	.04590						
.12000	.04736						
.13000	.04875						
.14000	.05006						
.15000	.05127						
.16000	.05242						
.17000	.05349						
.18000	.05454						
.19000	.05554						
.20000	.05648						
.22000	.05824						
.24000	.05984						
.26000	.06124						
.28000	.06250						
.30000	.06365						
.32000	.06466						
.34000	.06555						
.36000	.06636						
.38000	.06703						
.42000	.06811						
.46000	.06879						
.50000	.06904						
.52000	.06898						
.54000	.06885						
.56000	.06861						
.58000	.06821						
.60000	.06772						
.62000	.06707						
.64000	.06627						
.66000	.06537						
.68000	.06432						
.70000	.06313						
.72000	.06180						

ORIGINAL PAGE IS
OF POOR QUALITY

Table 3. Continued

.74000	.06032							
.76000	.05865							
.78000	.05680							
.80000	.05471							
.82000	.05242							
.84000	.04987							
.86000	.04715							
.88000	.04411							
.90000	.04080							
.92000	.03718							
.94000	.03324							
.96000	.02888							
.98000	.02413							
1.00000	.01896							
lower surface								
0.00000	0.00000							
.00200	-.00893							
.00500	-.01375							
.01000	-.01849							
.02000	-.02405							
.03000	-.02764							
.04000	-.03040							
.05000	-.03267							
.06000	-.03461							
.07000	-.03635							
.08000	-.03787							
.09000	-.03922							
.10000	-.04041							
.11000	-.04146							
.12000	-.04243							
.13000	-.04331							
.14000	-.04411							
.15000	-.04483							
.16000	-.04551							
.17000	-.04610							
.18000	-.04659							
.19000	-.04704							
.20000	-.04744							
.22000	-.04808							
.24000	-.04850							
.26000	-.04881							
.28000	-.04898							
.30000	-.04894							
.32000	-.04879							
.34000	-.04850							
.36000	-.04802							
.38000	-.04734							
.42000	-.04555							
.46000	-.04300							
.50000	-.03959							
.52000	-.03753							
.54000	-.03513							
.56000	-.03242							
.58000	-.02941							
.60000	-.02613							
.62000	-.02262							
.64000	-.01900							
.66000	-.01527							
.68000	-.01147							
.70000	-.00767							
.72000	-.00388							
.74000	-.00017							
.76000	.00344							
.78000	.00697							
.80000	.01022							
.82000	.01323							
.84000	.01588							
.86000	.01815							
.88000	.01988							
.90000	.02100							
.92000	.02140							
.94000	.02093							
.96000	.01937							
.98000	.01669							
1.00000	.01263							
zlin	xlin	ylin	chin	th	alin	fsec	fint	
20.95000	14.39000	0.00000	4.06000	1.00000	0.00000	1.00000	0.00000	
ysym	fnul	fnli						
0.00000	60.00000	60.00000						
trl	slt	xsing	ysing					
0.00000	0.00000	0.00000	0.00000					
upper surface								
0.00000	0.00000							
.00200	.00804							
.00500	.01254							
.01000	.01720							
.02000	.02349							
.03000	.02789							

Table 3. Continued

.04000	.03129
.05000	.03417
.06000	.03666
.07000	.03889
.08000	.04088
.09000	.04271
.10000	.04442
.11000	.04604
.12000	.04754
.13000	.04901
.14000	.05035
.15000	.05164
.16000	.05284
.17000	.05398
.18000	.05507
.19000	.05613
.20000	.05715
.22000	.05901
.24000	.06073
.26000	.06224
.28000	.06364
.30000	.06491
.32000	.06603
.34000	.06705
.36000	.06797
.38000	.06877
.42000	.07012
.46000	.07105
.50000	.07156
.52000	.07165
.54000	.07166
.56000	.07157
.58000	.07133
.60000	.07097
.62000	.07046
.64000	.06983
.66000	.06907
.68000	.06819
.70000	.06717
.72000	.06599
.74000	.06466
.76000	.06317
.78000	.06144
.80000	.05955
.82000	.05743
.84000	.05506
.86000	.05252
.88000	.04965
.90000	.04654
.92000	.04310
.94000	.03931
.96000	.03513
.98000	.03049
1.00000	.02541
lower surface	
0.00000	0.00000
.00200	-.00848
.00500	-.01331
.01000	-.01800
.02000	-.02345
.03000	-.02693
.04000	-.02959
.05000	-.03174
.06000	-.03360
.07000	-.03524
.08000	-.03668
.09000	-.03794
.10000	-.03907
.11000	-.04007
.12000	-.04097
.13000	-.04177
.14000	-.04250
.15000	-.04316
.16000	-.04374
.17000	-.04425
.18000	-.04468
.19000	-.04505
.20000	-.04539
.22000	-.04586
.24000	-.04614
.26000	-.04630
.28000	-.04632
.30000	-.04615
.32000	-.04587
.34000	-.04541
.36000	-.04481
.38000	-.04403
.42000	-.04198

ORIGINAL PAGE IS
OF POOR QUALITY

Table 3. Continued

ORIGINAL PAGE IS
OF POOR QUALITY

.46000	-.03917						
.50000	-.03549						
.52000	-.03331						
.54000	-.03080						
.56000	-.02800						
.58000	-.02492						
.60000	-.02154						
.62000	-.01799						
.64000	-.01431						
.66000	-.01048						
.68000	-.00660						
.70000	-.00269						
.72000	.00121						
.74000	.00501						
.76000	.00877						
.78000	.01243						
.80000	.01582						
.82000	.01894						
.84000	.02175						
.86000	.02411						
.88000	.02597						
.90000	.02721						
.92000	.02771						
.94000	.02738						
.96000	.02593						
.98000	.02331						
1.00000	.01935						
zlin	xlin	ylin	chin	th	alin	fsec	fint
22.95000	15.62000	0.000000	3.71000	1.00000	0.00000	1.00000	0.00000
ysym	fnui	fnli					
0.00000	60.00000	60.00000					
trl	slt	xsing	ysing				
0.00000	0.00000	0.00000	0.00000				
upper	surface						
0.00000	0.00000						
.00200	.00837						
.00500	.01278						
.01000	.01733						
.02000	.02347						
.03000	.02780						
.04000	.03120						
.05000	.03408						
.06000	.03661						
.07000	.03886						
.08000	.04093						
.09000	.04283						
.10000	.04464						
.11000	.04632						
.12000	.04792						
.13000	.04942						
.14000	.05085						
.15000	.05221						
.16000	.05349						
.17000	.05471						
.18000	.05588						
.19000	.05701						
.20000	.05810						
.22000	.06012						
.24000	.06199						
.26000	.06368						
.28000	.06522						
.30000	.06667						
.32000	.06795						
.34000	.06912						
.36000	.07021						
.38000	.07119						
.42000	.07285						
.46000	.07414						
.50000	.07500						
.52000	.07528						
.54000	.07548						
.56000	.07554						
.58000	.07550						
.60000	.07532						
.62000	.07503						
.64000	.07460						
.66000	.07405						
.68000	.07335						
.70000	.07253						
.72000	.07154						
.74000	.07043						
.76000	.06912						
.78000	.06761						
.80000	.06594						
.82000	.06403						
.84000	.06192						
.86000	.05960						
.88000	.05695						

Table 3. Continued

.90000	.05406						
.92000	.05086						
.94000	.04729						
.96000	.04327						
.98000	.03879						
1.00000	.03384						
lower surface							
0.00000	0.00000						
.00200	-.00798						
.00500	-.01275						
.01000	-.01742						
.02000	-.02270						
.03000	-.02605						
.04000	-.02854						
.05000	-.03059						
.06000	-.03231						
.07000	-.03383						
.08000	-.03517						
.09000	-.03635						
.10000	-.03738						
.11000	-.03827						
.12000	-.03909						
.13000	-.03978						
.14000	-.04045						
.15000	-.04101						
.16000	-.04151						
.17000	-.04190						
.18000	-.04222						
.19000	-.04251						
.20000	-.04274						
.22000	-.04302						
.24000	-.04312						
.26000	-.04305						
.28000	-.04288						
.30000	-.04254						
.32000	-.04207						
.34000	-.04146						
.36000	-.04067						
.38000	-.03974						
.42000	-.03736						
.46000	-.03420						
.50000	-.03018						
.52000	-.02782						
.54000	-.02519						
.56000	-.02224						
.58000	-.01906						
.60000	-.01560						
.62000	-.01194						
.64000	-.00817						
.66000	-.00424						
.68000	-.00023						
.70000	.00382						
.72000	.00785						
.74000	.01180						
.76000	.01573						
.78000	.01954						
.80000	.02312						
.82000	.02643						
.84000	.02937						
.86000	.03191						
.88000	.03391						
.90000	.03532						
.92000	.03595						
.94000	.03577						
.96000	.03446						
.98000	.03192						
1.00000	.02807						
zlin	xlin	ylin	chin	th	alin	fsec	fint
25.45000	17.18000	0.000000	3.27000	1.00000	0.00000	1.00000	0.00000
ysym	fnui	fnli					
0.00000	60.00000	60.00000					
trl	sit	xsing	ysing				
0.00000	0.00000	0.00000	0.00000				
upper surface							
0.00000	0.00000						
.00200	.00875						
.00500	.01310						
.01000	.01754						
.02000	.02345						
.03000	.02769						
.04000	.03105						
.05000	.03397						
.06000	.03656						
.07000	.03892						
.08000	.04108						
.09000	.04310						
.10000	.04504						
.11000	.04685						

ORIGINAL PAGE IS
OF POOR QUALITY

Table 3. Continued

.12000	.04857
.13000	.05021
.14000	.05177
.15000	.05326
.16000	.05464
.17000	.05599
.18000	.05731
.19000	.05858
.20000	.05977
.22000	.06205
.24000	.06420
.26000	.06618
.28000	.06799
.30000	.06969
.32000	.07126
.34000	.07268
.36000	.07403
.38000	.07527
.42000	.07753
.46000	.07938
.50000	.08084
.52000	.08143
.54000	.08190
.56000	.08228
.58000	.08254
.60000	.08270
.62000	.08271
.64000	.08263
.66000	.08239
.68000	.08203
.70000	.08154
.72000	.08089
.74000	.08010
.76000	.07912
.78000	.07797
.80000	.07666
.82000	.07510
.84000	.07336
.86000	.07143
.88000	.06916
.90000	.06665
.92000	.06382
.94000	.06060
.96000	.05688
.98000	.05269
1.00000	.04797
lower surface	
0.00000	0.00000
.00200	-.00711
.00500	-.01191
.01000	-.01649
.02000	-.02153
.03000	-.02464
.04000	-.02690
.05000	-.02872
.06000	-.03025
.07000	-.03161
.08000	-.03276
.09000	-.03378
.10000	-.03463
.11000	-.03542
.12000	-.03608
.13000	-.03662
.14000	-.03710
.15000	-.03749
.16000	-.03785
.17000	-.03808
.18000	-.03826
.19000	-.03837
.20000	-.03842
.22000	-.03841
.24000	-.03815
.26000	-.03777
.28000	-.03727
.30000	-.03661
.32000	-.03587
.34000	-.03496
.36000	-.03392
.38000	-.03271
.42000	-.02977
.46000	-.02604
.50000	-.02143
.52000	-.01882
.54000	-.01594
.56000	-.01278
.58000	-.00941
.60000	-.00577
.62000	-.00195

Table 3. Continued

.64000	.00199						
.66000	.00610						
.68000	.01031						
.70000	.01458						
.72000	.01885						
.74000	.02309						
.76000	.02730						
.78000	.03135						
.80000	.03525						
.82000	.03883						
.84000	.04203						
.86000	.04482						
.88000	.04712						
.90000	.04878						
.92000	.04968						
.94000	.04973						
.96000	.04863						
.98000	.04631						
1.00000	.04264						
zlin	xlin	ylin	chin	th	alin	fsec	fint
26.54000	17.81000	0.00000	3.12000	1.00000	0.00000	1.00000	0.00000
ysym	fnui	fnli					
0.00000	60.00000	60.00000					
trl	slt	xsing	ysing				
0.00000	0.00000	0.00000	0.00000				
upper surface							
0.00000	0.00000						
.00200	.00902						
.00500	.01329						
.01000	.01765						
.02000	.02344						
.03000	.02764						
.04000	.03098						
.05000	.03392						
.06000	.03653						
.07000	.03895						
.08000	.04116						
.09000	.04327						
.10000	.04526						
.11000	.04716						
.12000	.04896						
.13000	.05065						
.14000	.05231						
.15000	.05385						
.16000	.05533						
.17000	.05672						
.18000	.05812						
.19000	.05947						
.20000	.06074						
.22000	.06315						
.24000	.06544						
.26000	.06758						
.28000	.06952						
.30000	.07139						
.32000	.07313						
.34000	.07470						
.36000	.07620						
.38000	.07761						
.42000	.08016						
.46000	.08237						
.50000	.08413						
.52000	.08489						
.54000	.08556						
.56000	.08609						
.58000	.08655						
.60000	.08685						
.62000	.08706						
.64000	.08717						
.66000	.08711						
.68000	.08696						
.70000	.08664						
.72000	.08616						
.74000	.08559						
.76000	.08478						
.78000	.08384						
.80000	.08275						
.82000	.08139						
.84000	.07986						
.86000	.07814						
.88000	.07610						
.90000	.07378						
.92000	.07118						
.94000	.06814						
.96000	.06462						
.98000	.06056						
1.00000	.05598						
lower surface							
0.00000	0.00000						

ORIGINAL PAGE IS
OF POOR QUALITY

Table 3. Continued

.00200	-.00672		
.00500	-.01152		
.01000	-.01602		
.02000	-.02092		
.03000	-.02392		
.04000	-.02604		
.05000	-.02778		
.06000	-.02920		
.07000	-.03042		
.08000	-.03148		
.09000	-.03241		
.10000	-.03321		
.11000	-.03388		
.12000	-.03446		
.13000	-.03493		
.14000	-.03531		
.15000	-.03563		
.16000	-.03588		
.17000	-.03602		
.18000	-.03608		
.19000	-.03611		
.20000	-.03610		
.22000	-.03589		
.24000	-.03548		
.26000	-.03492		
.28000	-.03423		
.30000	-.03340		
.32000	-.03249		
.34000	-.03140		
.36000	-.03019		
.38000	-.02885		
.42000	-.02560		
.46000	-.02158		
.50000	-.01662		
.52000	-.01384		
.54000	-.01082		
.56000	-.00753		
.58000	-.00405		
.60000	-.00032		
.62000	.00361		
.64000	.00763		
.66000	.01188		
.68000	.01622		
.70000	.02062		
.72000	.02502		
.74000	.02942		
.76000	.03376		
.78000	.03800		
.80000	.04205		
.82000	.04581		
.84000	.04919		
.86000	.05211		
.88000	.05455		
.90000	.05639		
.92000	.05740		
.94000	.05762		
.96000	.05668		
.98000	.05444		
1.00000	.05091		
fnf	fcirc		
20.00000	0.00000		
fnfp	xf	fsec	
1.00000	-17.56000	1.00000	
yf	zf		
0.00000	0.00000		
fnfp	xf(i)	fsec	
41.	-17.16000	1.	
yf	zf		
.60100	0.00000		
.60025	.03005		
.59799	.06010		
.59420	.09015		
.58886	.12020		
.58192	.15025		
.57332	.18030		
.56299	.21035		
.55083	.24040		
.53671	.27045		
.52048	.30050		
.50193	.33055		
.48080	.36060		
.45672	.39065		
.42920	.42070		
.39752	.45075		
.36060	.48080		
.31660	.51085		
.26197	.54090		
.18766	.57095		

Table 3. Continued

.00000	.60100		
-.18766	.57095		
-.26197	.54090		
-.31660	.51085		
-.36060	.48080		
-.39752	.45075		
-.42920	.42070		
-.45672	.39065		
-.48080	.36060		
-.50193	.33055		
-.52048	.30050		
-.53671	.27045		
-.55083	.24040		
-.56299	.21035		
-.57332	.18030		
-.58192	.15025		
-.58886	.12020		
-.59420	.09015		
-.59799	.06010		
-.60025	.03005		
-.60100	-.00000		
fnfp	xf	fsec	
2.00000	-16.96000	0.00000	
yf	zf		
.73000	0.00000		
-.73000	0.00000		
fnfp	xf	fsec	
2.00000	-16.56000	0.00000	
yf	zf		
.97400	0.00000		
-.97400	0.00000		
fnfp	xf	fsec	
2.00000	-15.56000	0.00000	
yf	zf		
1.50700	0.00000		
-1.50700	0.00000		
fnfp	xf	fsec	
2.00000	-14.56000	0.00000	
yf	zf		
1.94000	0.00000		
-1.94000	0.00000		
fnfp	xf	fsec	
2.00000	-13.56000	0.00000	
yf	zf		
2.28400	0.00000		
-2.28400	0.00000		
fnfp	xf	fsec	
2.00000	-12.56000	0.00000	
yf	zf		
2.54600	0.00000		
-2.54600	0.00000		
fnfp	xf	fsec	
2.00000	-11.56000	0.00000	
yf	zf		
2.73000	0.00000		
-2.73000	0.00000		
fnfp	xf	fsec	
2.00000	-10.56000	0.00000	
yf	zf		
2.83900	0.00000		
-2.83900	0.00000		
fnfp	xf	fsec	
2.00000	-9.56000	0.00000	
yf	zf		
2.87500	0.00000		
-2.87500	0.00000		
fnfp	xf	fsec	
2.0	-2.0	0.	
yf	zf		
2.87500	0.00		
-2.87500	0.000		
fnfp	xf	fsec	
2.00000	19.44000	0.00000	
yf	zf		
2.79500	0.00000		
-2.79500	0.00000		
fnfp	xf	fsec	
2.00000	21.44000	0.00000	
yf	zf		
2.73000	0.00000		
-2.73000	0.00000		
fnfp	xf	fsec	
2.00000	23.44000	0.00000	
yf	zf		
2.64600	0.00000		
-2.64600	0.00000		
fnfp	xf	fsec	
2.00000	25.44000	0.00000	

ORIGINAL PAGE IS
OF POOR QUALITY

Table 3. Concluded

ORIGINAL PAGE IS
OF POOR QUALITY

yf	zf	
2.54300	0.00000	
-2.54300	0.00000	
fnfp	xf	fsec
2.00000	27.44000	0.00000
yf	zf	
2.42100	0.00000	
-2.42100	0.00000	
fnfp	xf	fsec
2.00000	29.44000	0.00000
yf	zf	
2.27900	0.00000	
-2.27900	0.00000	
fnfp	xf	fsec
2.00000	31.44000	0.00000
yf	zf	
2.11900	0.00000	
-2.11900	0.00000	
fnfp	xf	fsec
2.00000	32.44000	0.00000
yf	zf	
2.03000	0.00000	
-2.03000	0.00000	

Table 4. Description of Inviscid-Iteration and Global-Interaction Control Variables for Unit 5

<u>Read order</u>	<u>Number of records</u>	<u>Description and comments</u>
<u>INVISCID CALCULATION INPUT</u> (Read in subroutine FLO30)		
1	1	TITLE. - Descriptive title of inviscid calculation. This title appears on the formatted output on unit 6. FORMAT (8A10)
2	1	DESC. - Description for record in read order 3.
3	1	FNX, FNY, FNZ, FMESH, VIS, QC FORMAT (8E10.7) FNX. - Number of inviscid computational grid points in the "chordwise direction" from downstream boundary, around the leading edge, and back to downstream boundary. Maximum is 160 and FNX must be a multiple of 20. FNX is set to less than 1.0 to terminate calculations. FNY. - Number of inviscid computational grid points in "normal direction" from airfoil surface to outer boundary. Maximum is 24 and FNY must be a multiple of 3. FNZ. - Number of inviscid computational grid points in "spanwise direction" from fuselage across wing semispan to maximum distance off the wingtip. Maximum is 32 and FNZ must be a multiple of 4. FMESH. - Number of meshes on which solutions are desired. After the solution is obtained on each grid, the number of mesh cells in each coordinate direction is doubled, and a new solution is computed. The converged solution on each grid is interpolated to the next grid and used as the initial estimates for the solution on the next grid. FMESH refers to grid refinement, not multigrid. VIS. - Governs whether the first- or second-order artificial viscosity is used in the inviscid solver. VIS = 0. Original FLO30 first-order viscosity is used. VIS = 1. Second-order viscosity is used.

Table 4. Continued

<u>Read order</u>	<u>Number of records</u>	<u>Description and comments</u>
		QC - Square of the switch Mach number above which the artificial viscosity is added. It is chosen to be slightly less than 1.0 for best performance; use 0.9 for difficult cases.
4	1	DESC. - Description for record in read order 5.
5	1	FPLOT, FCONT, BLCF
		<p>FPLOT. - Inviscid-iteration output trigger FPLOT = 0. Minimum output. Postprocessor plotting data are not written to TAPE 1, printer C_p plots are not generated, and input wing and fuselage data are not printed out.</p> <p>FPLOT = 1. Postprocessor plotting data are written to TAPE 1.</p> <p>FPLOT = 2. Postprocessor plotting data are written to TAPE 1, and printer C_p plots are generated.</p> <p>FPLOT = 3. Postprocessor plotting data are written to TAPE 1, printer C_p plots are generated, and input wing and fuselage data are printed out.</p> <p>FCONT. - Program starting/restarting trigger.</p> <p>FCONT = 0. Inviscid calculation begins at iteration zero with potential and boundary-layer (B.L.) quantities equal to zero everywhere.</p> <p>FCONT = 1. Inviscid calculation begins at iteration zero with potential equal to zero. Previously calculated values of B.L. quantities are used.</p> <p>FCONT = 2. Inviscid calculation continues from previously obtained values of potential. Previously obtained values of B.L. quantities are used.</p>

Table 4. Continued

<u>Read order</u>	<u>Number of records</u>	<u>Description and comments</u>
		<p>FCONT = 3. Inviscid calculation continues from previously obtained values of potential which are read in from the restart file for unit 4. Previously obtained values of B.L. quantities (read from restart file for unit 4) are used. For restart, FNX, FNY, and FNZ must correspond to values of data on the restart file. Restart is on fine grid only.</p> <p>BLCP. - B.L. control parameter for <u>inviscid</u> iterations.</p> <p>BLCP = 0.0. No viscous corrections are applied on wing or wake.</p> <p>BLCP = 1.0. Displacement thickness B.L. correction is applied on wing. No <u>viscous</u> wake treatment is applied, but the boundary conditions in the wake are different from those in original FLO30 program. (Wake calculation is not performed and not used.) The enforced wake boundary conditions are: strict flow tangency at vortex wake sheet and no jump in pressure across the wake.</p> <p>BLCP = 1.5. Same as BLCP = 1.0 except that wake calculation is performed but not used. BLCP = 1.5 is used if next global iteration will use BLCP = 2.0 or 3.0.</p> <p>BLCP = 2.0. Displacement thickness B.L. correction is applied on wing and wake. (No wake-curvature effects included.)</p> <p>BLCP = 3.0. Same as BLCP = 2.0.</p>
6	1	DESC. - Description of record in read order 7.
7	1	FIX, FIY, FIXO, FINNR
		<p>FIX. - Number of complete multigrid cycles using XSWEEP.</p>

Table 4. Continued

<u>Read order</u>	<u>Number of records</u>	<u>Description and comments</u>
		<p>FIY. - Number of complete multigrid cycles using YSWEEP.</p> <p>FIXO. - FIXO = 0. Multigrid process starts with XSWEEP.</p> <p style="padding-left: 40px;">FIXO = 1. Multigrid process starts with YSWEEP.</p> <p>FINNR. - FINNR = 0. The same relaxation scheme is used throughout a multigrid cycle (either XSWEEP or YSWEEP).</p> <p style="padding-left: 40px;">FINNR = 1. One XSWEEP and one YSWEEP sweep are used on each grid in the multigrid cycle (explicit alternating direction).</p>
8	1	DESC. - Description for record(s) in read order 9.
9	1 record for each grid on which solution is to be obtained (FMESH)	<p>TOTO, COVO, P10, P20, P30, GMESH, FIT10, FIT20</p> <p>FORMAT (8E10.7)</p> <p>TOTO. - Maximum number of work units on this grid. (A work unit is equal to one fine-grid iteration using XSWEEP or YSWEEP.)</p> <p>COVO. - Convergence criterion on the average residual.</p> <p>P10. - Subsonic-point relaxation factor on this grid. P10 <u>must be < 2.</u>, typically 1.6, but may be reduced nearer to 1.0 for difficult cases.</p> <p>P20. - Supersonic-point relaxation factor on this grid. P20 <u>must be ≤ 1.</u> A value of 0.8 is a reasonable value.</p> <p>P30. - Circulation relaxation factor. P30 may be > 1.0, but a value of 1.0 is recommended. For lift specification, (FCL = 1.0) P30 should be 0.1 → 0.3.</p>

Table 4. Continued

<u>Read order</u>	<u>Number of records</u>	<u>Description and comments</u>
		<p>GMESH. - Number of meshes to be used in multigrid sequence. Must be less than or equal to $FNX/20$ so that the coarsest mesh in the multigrid sequence contains at least $20 \times 3 \times 4$ cells. (Example: If FNX, FNY, and FNZ are $160 \times 24 \times 32$, GMESH should be 4 so that the multigrid meshes are $160 \times 24 \times 32$, $80 \times 12 \times 16$, $40 \times 6 \times 8$, and $20 \times 3 \times 4$.)</p> <p>FIT10. - Number of relaxation sweeps on each grid (in multigrid) when coarsening. (Double sweeps, one XSWEET and one YSWEET, when $FINNR = 1.0$.) Increasing FIT10 usually helps the lift to converge more quickly, but may cause problems if the supersonic zone is too large.</p> <p>FIT20. - Number of relaxation sweeps on each grid after corrections from coarser grids have been added. (Double sweeps, one XSWEET and one YSWEET, when $FINNR = 1.0$.) Increasing FIT20 aids stability of the scheme, but it is expensive since it increases work on the finest grid in the multigrid cycle.</p>
10	1	DESC. - Description for record in read order 11.
11	1	<p>FMACH, ALDEG, CDO, FCL, CLSPEC FORMAT (8E10.7)</p> <p>FMACH. - Free-stream Mach number.</p> <p>ALDEG. - Angle of attack (in degrees) measured in plane containing free-stream direction. ALDEG is used as a starting angle if $FCL = 1.0$ (lift specification mode). Algorithm works best if ALDEG is nonzero for $FCL = 1.0$.</p> <p>CDO. - Optional subcritical drag coefficient. CDO is added to the calculated wave and vortex drag to give an estimate of the total drag (usually $CDO = 0.0$).</p> <p>FCL. - Lift specification parameter. $FCL = 0.0$ indicates that angle of attack is specified.</p> <p>FCL = 1.0 indicates that program will adjust the angle of attack (starting with ALDEG) so that the lift based on the circulation matches CLSPEC. This will cause the lift based on the integrated pressures on the wing to approximately match CLSPEC.</p>

Table 4. Continued

<u>Read order</u>	<u>Number of records</u>	<u>Description and comments</u>
		CLSPEC. - Specified wing lift coefficient. CLSPEC is used only if FCL = 1.0.
		<u>BOUNDARY-LAYER CALCULATION INPUT</u> (Read in subroutine EINLES)
12	2	TITLE. - Identification title used on printout and plots. FORMAT (20A4/20A4)
13	1	DESC. - Description for record in read order 14.
14	1	UINF, RINF, AK(1), AK(2), XDRUCK FORMAT (9F10.5) UINF. - Reference velocity. Its value is usually unimportant. (Used only on scale surface velocity in output for IPRINT = 2.0.) UNIF = 0.0 will skip the viscous calculation. This may be used to run the code in purely inviscid mode. RINF. - Free-stream unit Reynolds number (in millions per unit length). (Unit length must be in same unit as geometry definition.) AK(1). - Upper-surface B.L. laminar-to-turbulent transition location (in chord fraction). AK(2). - Lower-surface B.L. laminar-to-turbulent transition location (in chord fraction). XDRUCK. - Output step (in chord fraction). The output from the B.L. calculation is given at chord stations XDRUCK from each other. Results for the upper surface are given first, leading edge to trailing edge; and then the lower-surface results are given, leading edge to trailing edge.
15	1	DESC. - Description for record in read order 16.
16	1	XPROZF(1), XPROZF(2), XPROZR(1), XPROZR(2) XPROZF(1). - Forward limit of boundary-layer starting location—upper surface. XPROZF(2). - Forward limit of boundary-layer starting location—lower surface.

Table 4. Continued

<u>Read order</u>	<u>Number of records</u>	<u>Description and comments</u>
		XPROZR(1). - Rearward limit of boundary-layer starting location—upper surface.
		XPROZR(2). - Rearward limit of boundary-layer starting location—lower surface.
		NOTE: If XPROZR(1) or XPROZR(2) is 0.0, the program will automatically calculate the boundary-layer starting-location information.
17	1	DESC. - Description for record in read order 18.
18	1	FFLAG, FFIPRNT FORMAT (8F10.6)
		FFLAG. - Lag-entrainment control parameter.
		FFLAG = 0. No lag entrainment in wing B.L.
		FFLAG = 1.0. Lag entrainment included in wing B.L. calculation. For high N_{Re} , lag-entrainment effects are small. FFLAG = 1.0 may be destabilizing for high N_{Re} where the lag-entrainment model used in the code is not valid.
		FFIPRN. - B.L. print control parameter.
		FFIPRN = -2.0. Print δ^* on upper and lower surfaces at the B.L. computational points and short map at the hard geometric points. Print δ^* at inviscid computational points (AUSGB).
		FFIPRN = -1.0. Print δ^* on upper and lower surfaces at the B.L. computational points and short map of δ^* at hard geometric points.
		FFIPRN = 0.0. Shortest printout δ^* at B.L. computational points (recommended for most runs).
		FFIPRN = 1.0. Print inviscid velocities used to drive the B.L. calculations at the inviscid grid points. Print on upper and lower surfaces at the B.L. computational points and short map of δ^* at hard geometric points.

Table 4. Concluded

<u>Read order</u>	<u>Number of records</u>	<u>Description and comments</u>
		FFIPRNT = 2.0. Print inviscid velocities used to drive the B.L. calculations at inviscid grid points. Print δ^* on upper and lower surfaces at the B.L. computational points and short map at the hard geometric points. Print δ^* at inviscid computational points (AUSGB). (This print option generates an extremely large amount of output and should be used <u>only</u> when necessary.)

BOUNDARY-LAYER TO INVISCID INTERPOLATION PARAMETERS

(Read in subroutine EINLES)

19	1	DESC. - Description for record in read order 20.
20	1	<p>RELI, FISEPE(1), FISEPE(2) FORMAT (3F10.0)</p> <p>RELI. - Relaxation factor for δ^* corrections in interaction. RELI must be ≤ 1.0. A value of 0.5 is recommended.</p> <p>FISEPE(1). - Upper-surface linear-extrapolation flag. Transitory regions of separation in initial global iteration may cause instabilities. Constant value extrapolation of δ^* is used through the region of separation if FISEPE $\neq 0.0$. (Use FISEPE = 1.0.) Near convergence, FISEPE must be equal to 0.0.</p> <p>FISEPE(2). - Same as FISEPE(1) except for the lower surface.</p>

Read orders 1-20 define a single global iteration. Repeated global iterations are performed by repetition of blocks of read orders 1-20. The program terminates by reading the first three read orders with FNX < 1.0; that is, the last three records should be:

1	1	TITLE. - End of calculation.
2	1	DESC. - Description for record in read order 3.
3	1	0.0

Table 5. Sample Input File of Inviscid-Iteration and Global-Interaction Control Parameters for Unit 5

```

PF I - smoothed - Test 14, Run 49 - viscous iter1
  fnx    fny    fnz    fmesh    vis    qc
  40.    6.     8.     3.0     0.0   .95
  fplot  fcont  blcp
  0.     0.     0.
  fix    fiy    fix0   finnr
  1.0    1.0    0.0    1.0
  fit    cov0  p10    p20    p30   gmesh  fit10  fit20
  40.    1.e-06  1.0    .6     1.    2.     2.0    2.0
  30.    1.e-06  1.0    .6     1.    3.     2.0    2.0
  20.    1.e-06  1.0    .6     1.    4.     2.0    2.0
  fmach  aldeg  cd0
  .801  2.00    0.000
Pathfinder I
  iter 1
    uinf  rinf(mil)  ak(1)  ak(2)  xdruck
    1.    3.00      0.00  0.00  .100
  xprozf(1) xprozf(2) xprozr(1) xprozr(2)
  0.0    0.0      0.0    0.0
  fflag  ffiprint
  0.0    0.0
  reli  fisepe(1) fisepe(2)
  -0.7  1.0      1.0
PF I - smoothed - Test 14, Run 49 - viscous iter2
  fnx    fny    fnz    fmesh    vis    qc
  160.   24.   32.   1.0     0.0   .95
  fplot  fcont  blcp
  0.     0.     1.
  fix    fiy    fix0   finnr
  1.0    1.0    0.0    1.0
  fit    cov0  p10    p20    p30   gmesh  fit10  fit20
  20.    1.e-06  1.0    .6     1.    4.     2.0    2.0
  fmach  aldeg  cd0
  .801  2.00    0.000
Pathfinder I
  iter 2
    uinf  rinf(mil)  ak(1)  ak(2)  xdruck
    1.    3.00      0.00  0.00  .100
  xprozf(1) xprozf(2) xprozr(1) xprozr(2)
  0.0    0.0      0.0    0.0
  fflag  ffiprint
  0.0    0.0
  reli  fisepe(1) fisepe(2)
  .4     1.0      1.0
PF I - smoothed - Test 14, Run 49 - viscous iter3
  fnx    fny    fnz    fmesh    vis    qc
  160.   24.   32.   1.0     0.0   .95
  fplot  fcont  blcp
  0.     2.     1.5
  fix    fiy    fix0   finnr
  1.0    1.0    0.0    1.0
  fit    cov0  p10    p20    p30   gmesh  fit10  fit20
  20.    1.e-06  1.0    .6     1.    4.     2.0    2.0
  fmach  aldeg  cd0
  .801  2.00    0.000
Pathfinder I
  iter 3
    uinf  rinf(mil)  ak(1)  ak(2)  xdruck
    1.    3.00      0.02  0.02  .100
  xprozf(1) xprozf(2) xprozr(1) xprozr(2)
  0.0    0.0      0.0    0.0
  fflag  ffiprint
  0.0    0.0
  reli  fisepe(1) fisepe(2)
  .5     1.0      1.0
PF I - smoothed - Test 14, Run 49 - viscous iter4
  fnx    fny    fnz    fmesh    vis    qc
  160.   24.   32.   1.0     0.0   .95
  fplot  fcont  blcp
  0.     2.     2.
  fix    fiy    fix0   finnr
  1.0    1.0    0.0    1.0
  fit    cov0  p10    p20    p30   gmesh  fit10  fit20
  20.    1.e-06  1.0    .6     1.    4.     2.0    2.0
  fmach  aldeg  cd0
  .801  2.00    0.000
Pathfinder I
  iter 4

```

ORIGINAL PAGE IS
OF POOR QUALITY

Table 5. Continued

```

uinf rinf(mil)      ak(1)      ak(2)      xdruck
  1.      3.00      0.04      0.04      .100
xprozf(1) xprozf(2) xprozr(1) xprozr(2)
  0.0      0.0      0.0      0.0
fflag  ffiprint
  0.0      0.0
reli  fisepe(1) fisepe(2)
  .5      1.0      1.0
PF I - smoothed - Test 14, Run 49 - viscous iter5
  fnx      fny      fnz      fmesh      vis      qc
  160.     24.     32.     1.0      1.0      .95
fplot      fcont      blcp
  0.        2.        2.
fix        fiy        fix0      finnr
  1.0      1.0      0.0      1.0
fit        cov0      p10      p20      p30      gmesh      fit10      fit20
  20.     1.e-06     1.0     .6      1.        4.        2.0      2.0
fmach      aldeg      cd0
  .801     2.00     0.000
Pathfinder I
  iter 5
uinf rinf(mil)      ak(1)      ak(2)      xdruck
  1.      3.00      0.06      0.06      .100
xprozf(1) xprozf(2) xprozr(1) xprozr(2)
  0.0      0.0      0.0      0.0
fflag  ffiprint
  1.0     -1.0
reli  fisepe(1) fisepe(2)
  .5      1.0      1.0
PF 1 smooth (Test 14, Run 49) viscous iter6
  fnx      fny      fnz      fmesh      vis      qc
  160.     24.     32.     1.0      1.0      .95
fplot      fcont      blcp
  0.        2.        2.
fix        fiy        fix0      finnr
  1.0      1.0      0.0      1.0
fit        cov0      p10      p20      p30      gmesh      fit10      fit20
  20.     1.e-06     1.0     .6      1.        4.        2.0      2.0
fmach      aldeg      cd0
  .801     2.00     0.000
Pathfinder I
  iter 6
uinf rinf(mil)      ak(1)      ak(2)      xdruck
  1.      3.00      0.08      0.08      .100
xprozf(1) xprozf(2) xprozr(1) xprozr(2)
  0.0      0.0      0.0      0.0
fflag  ffiprint
  1.0      0.0
reli  fisepe(1) fisepe(2)
  .5      1.0      1.0
PF 1 smooth (Test 14, Run 49) viscous iter7
  fnx      fny      fnz      fmesh      vis      qc
  160.     24.     32.     1.0      1.0      .98
fplot      fcont      blcp
  0.        2.        2.
fix        fiy        fix0      finnr
  1.0      1.0      0.0      1.0
fit        cov0      p10      p20      p30      gmesh      fit10      fit20
  20.     1.e-06     1.0     .6      1.        4.        2.0      2.0
fmach      aldeg      cd0
  .801     2.00     0.000
Pathfinder I
  iter 7
uinf rinf(mil)      ak(1)      ak(2)      xdruck
  1.      3.00      0.10      0.10      .100
xprozf(1) xprozf(2) xprozr(1) xprozr(2)
  0.0      0.0      0.0      0.0
fflag  ffiprint
  1.0      0.0
reli  fisepe(1) fisepe(2)
  .5      1.0      1.0
PF 1 smooth (Test 14, Run 49) viscous iter8
  fnx      fny      fnz      fmesh      vis      qc
  160.     24.     32.     1.0      1.0      .98
fplot      fcont      blcp
  0.        2.        2.
fix        fiy        fix0      finnr
  1.0      1.0      0.0      1.0

```

Table 5. Concluded

```

fit      cov0      p10      p20      p30      gmesh      fit10      fit20
20.     1.e-06      1.0     .6      1.      4.      2.0     2.0
fmach    aldeg      cd0
.801    2.00     0.000

Pathfinder I
iter 8
  uinf rinf(mil)      ak(1)      ak(2)      xdruck
  1.      3.00     0.10     0.10     .100
xprozf(1) xprozf(2) xprozr(1) xprozr(2)
  0.0     0.0     0.0     0.0
  fflag ffiprint
  1.0     0.0
  reli fisepe(1) fisepe(2)
  .5      1.0     1.0
PF 1 smooth (Test 14, Run 49) viscous iter9
  fnx      fny      fnz      fmesh      vis      qc
  160.     24.     32.     1.0     1.0     .98
  fplot    fcont    blcp
  0.      2.      2.
  fix      fiy      fix0     finnr
  1.0     1.0     0.0     1.0
  fit      cov0      p10      p20      p30      gmesh      fit10      fit20
  20.     1.e-06      1.0     .6      1.      4.      2.0     2.0
  fmach    aldeg      cd0
  .801    2.00     0.000

Pathfinder I
iter 9
  uinf rinf(mil)      ak(1)      ak(2)      xdruck
  1.      3.00     0.10     0.10     .100
xprozf(1) xprozf(2) xprozr(1) xprozr(2)
  0.0     0.0     0.0     0.0
  fflag ffiprint
  1.0     0.0
  reli fisepe(1) fisepe(2)
  .5      1.0     1.0
PF 1 smooth (Test 14, Run 49) viscous iter10
  fnx      fny      fnz      fmesh      vis      qc
  160.     24.     32.     1.0     1.0     .98
  fplot    fcont    blcp
  0.      2.      2.
  fix      fiy      fix0     finnr
  1.0     1.0     0.0     1.0
  fit      cov0      p10      p20      p30      gmesh      fit10      fit20
  20.     1.e-06      1.0     .6      1.      4.      2.0     2.0
  fmach    aldeg      cd0
  .801    2.00     0.000

Pathfinder I
iter 10
  uinf rinf(mil)      ak(1)      ak(2)      xdruck
  1.      3.00     0.10     0.10     .100
xprozf(1) xprozf(2) xprozr(1) xprozr(2)
  0.0     0.0     0.0     0.0
  fflag ffiprint
  1.0     0.0
  reli fisepe(1) fisepe(2)
  .5      1.0     1.0
end of calculation
  fnx
  0.0

```

ORIGINAL PAGE IS
OF POOR QUALITY

ORIGINAL PAGE IS
OF POOR QUALITY

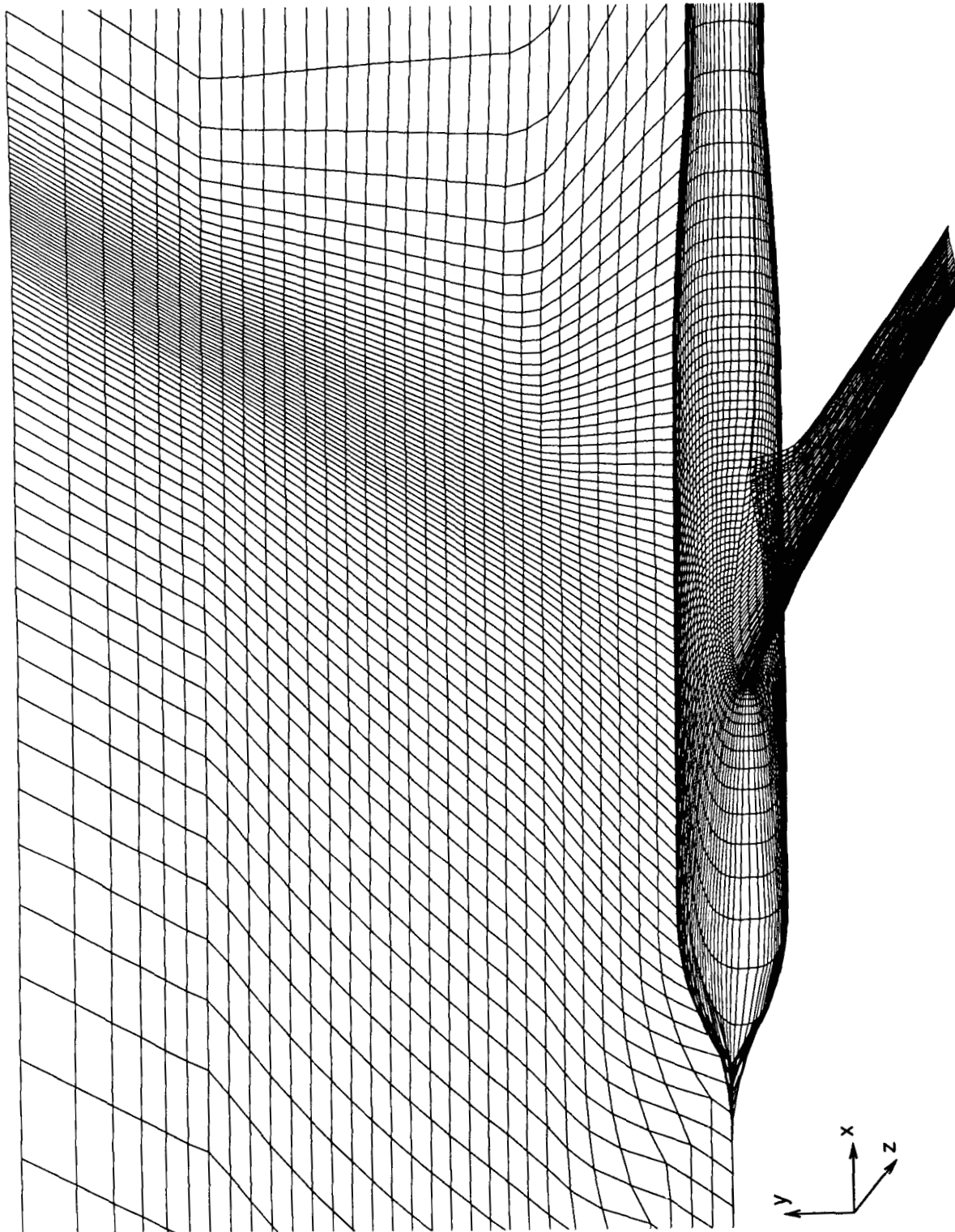
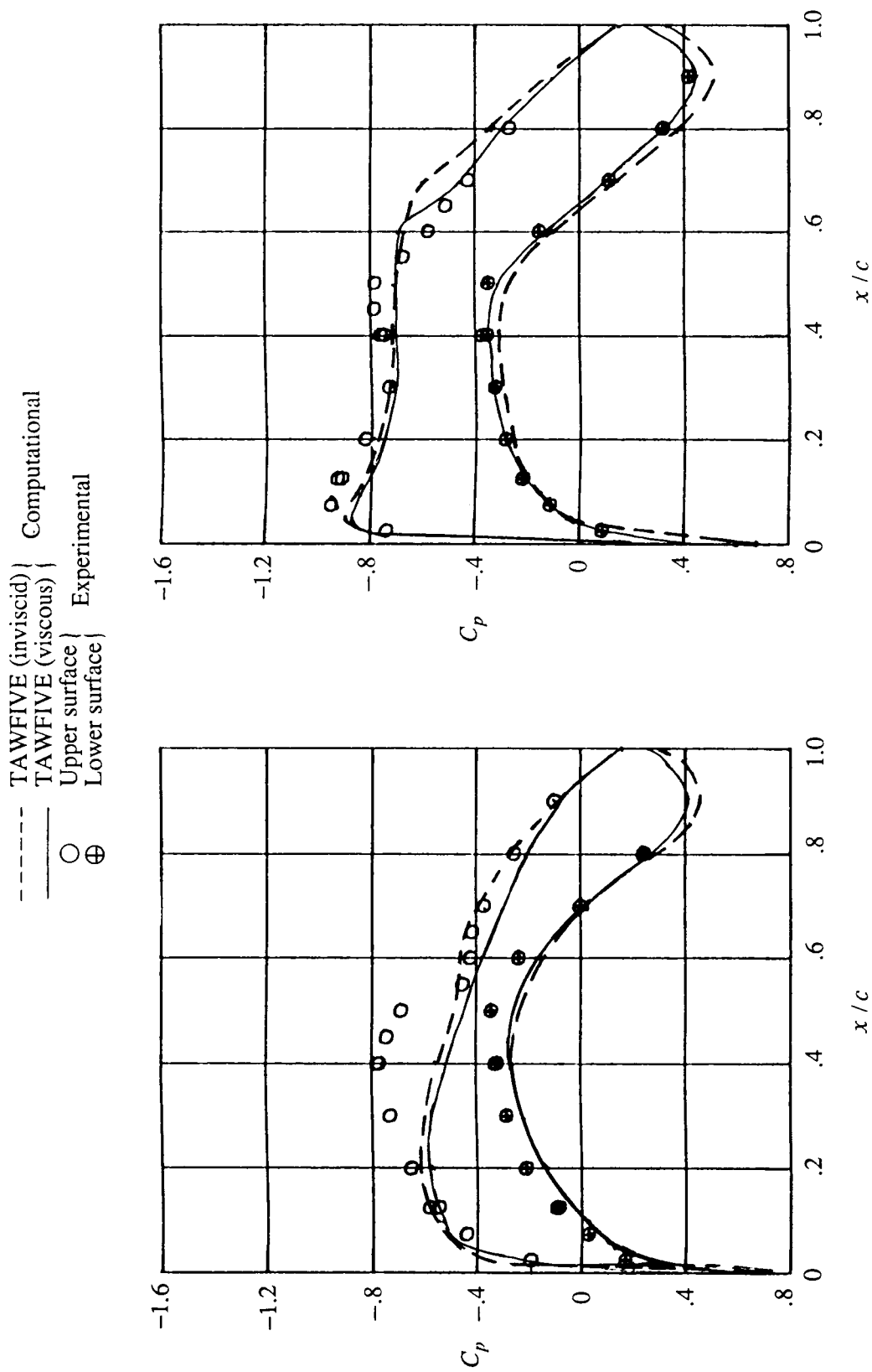


Figure 1. Portion of typical grid.

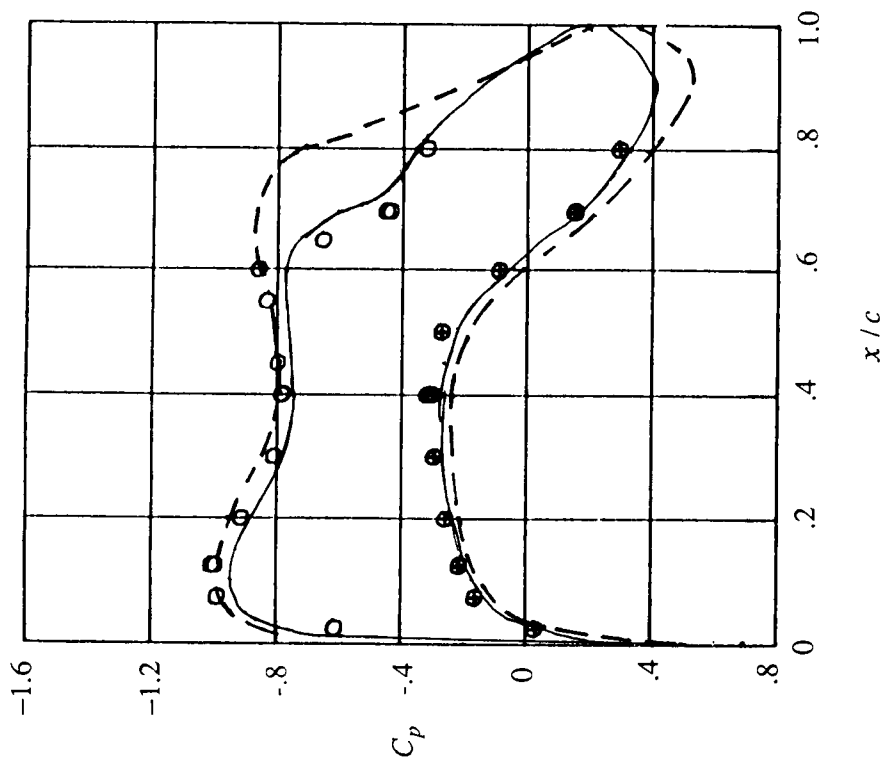


(a) $\eta = 0.13$.

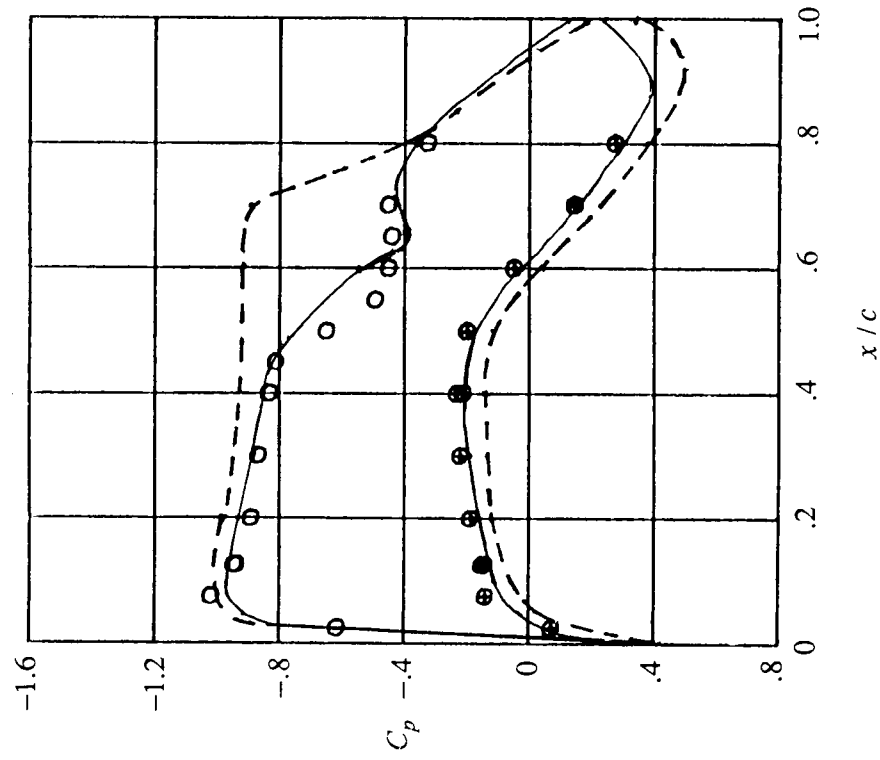
(b) $\eta = 0.28$.

Figure 2. Comparison of computational and experimental data for Pathfinder I at $M_\infty = 0.82$, $\alpha = 1.93^\circ$, and $N_{Re} = 17.0 \times 10^6$.

--- Computational
 --- Computational
 ○ Upper surface | Experimental
 ⊕ Lower surface | Experimental



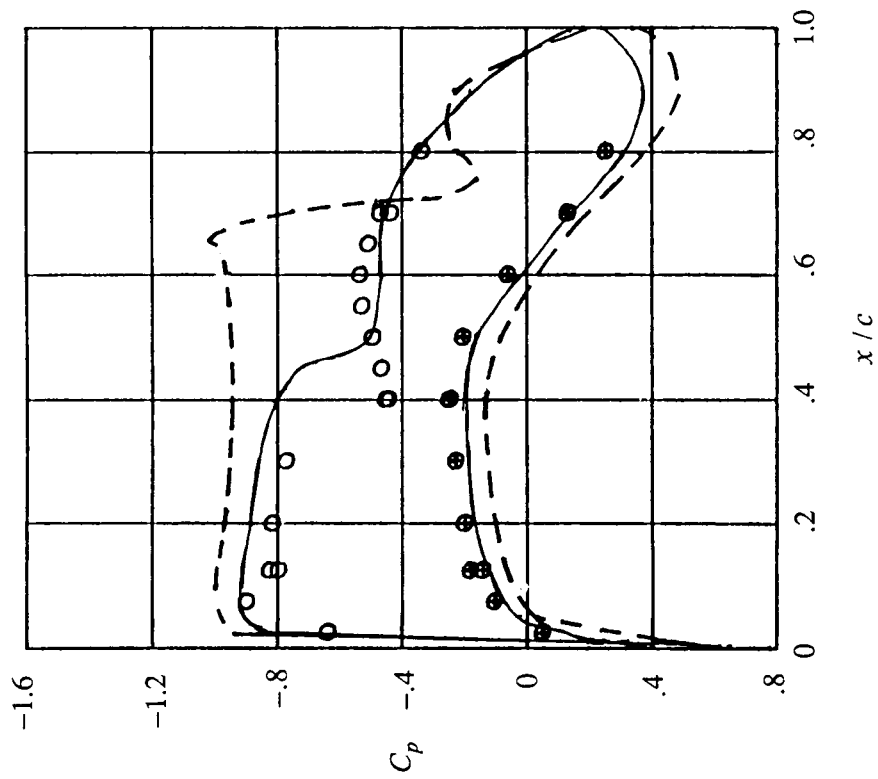
(c) $\eta = 0.43$.



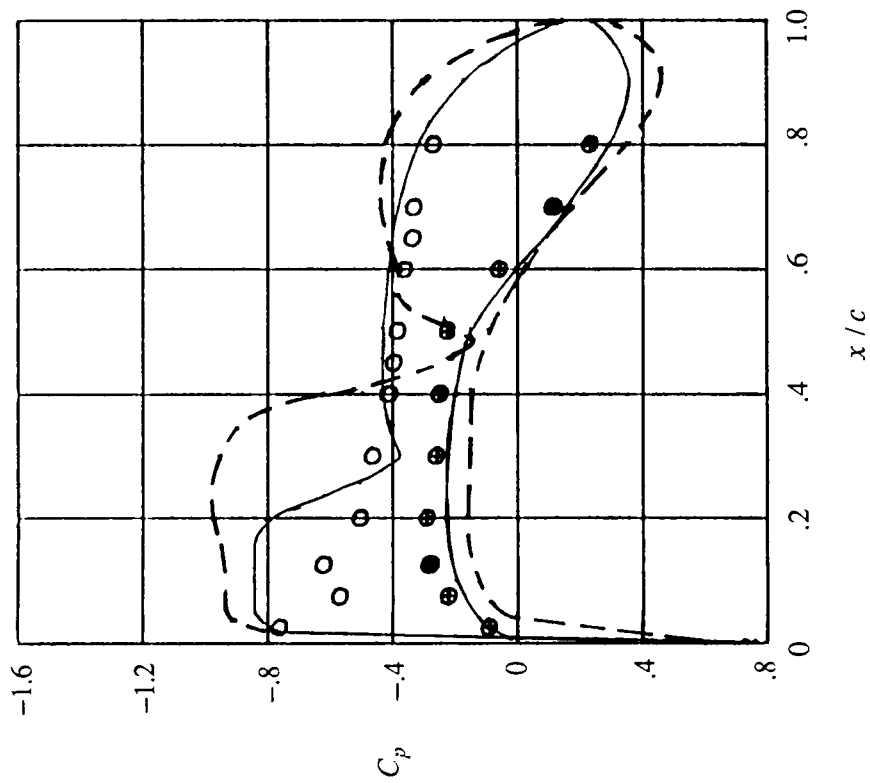
(d) $\eta = 0.64$.

Figure 2. Continued.

- - - TAWFIVE (inviscid) Computational
 — TAWFIVE (viscous) Computational
 ○ Upper surface Experimental
 ⊕ Lower surface Experimental



(e) $\eta = 0.83$.



(f) $\eta = 0.96$.

Figure 2. Concluded.

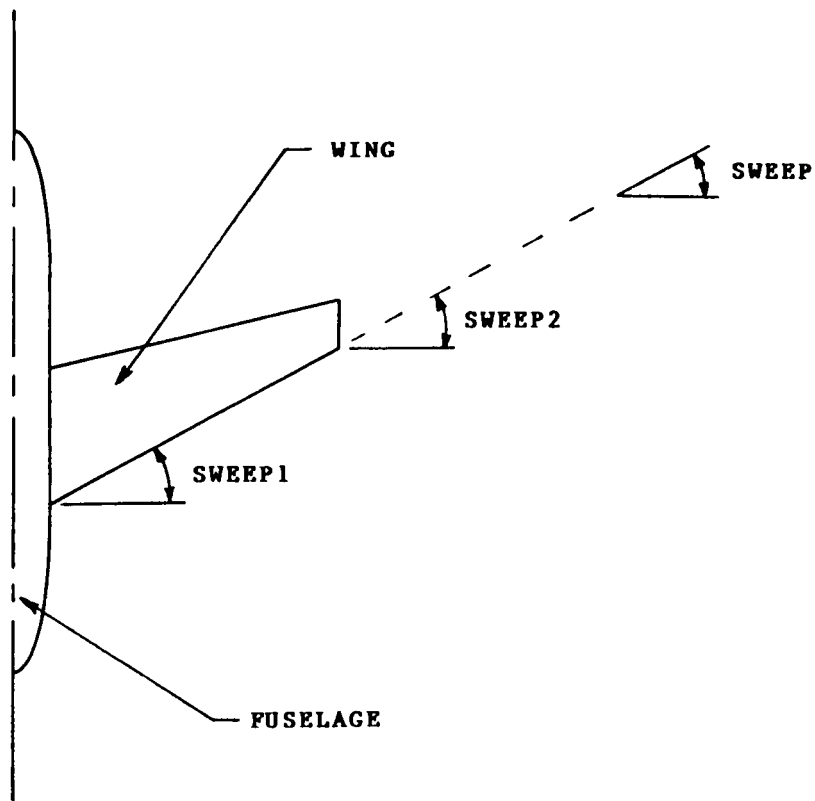


Figure 3. Definition of SWEEP1, SWEEP2, and SWEEP in read order 3. Dimensions and angles are exaggerated for clarity.

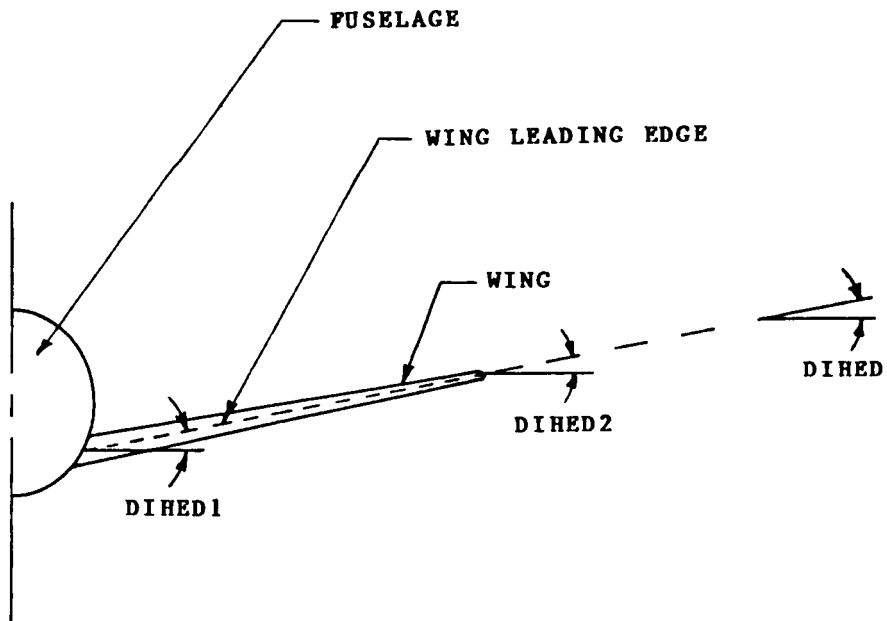


Figure 4. Definition of DIHED1, DIHED2, and DIHED in read order 3. Dimensions and angles are exaggerated for clarity.

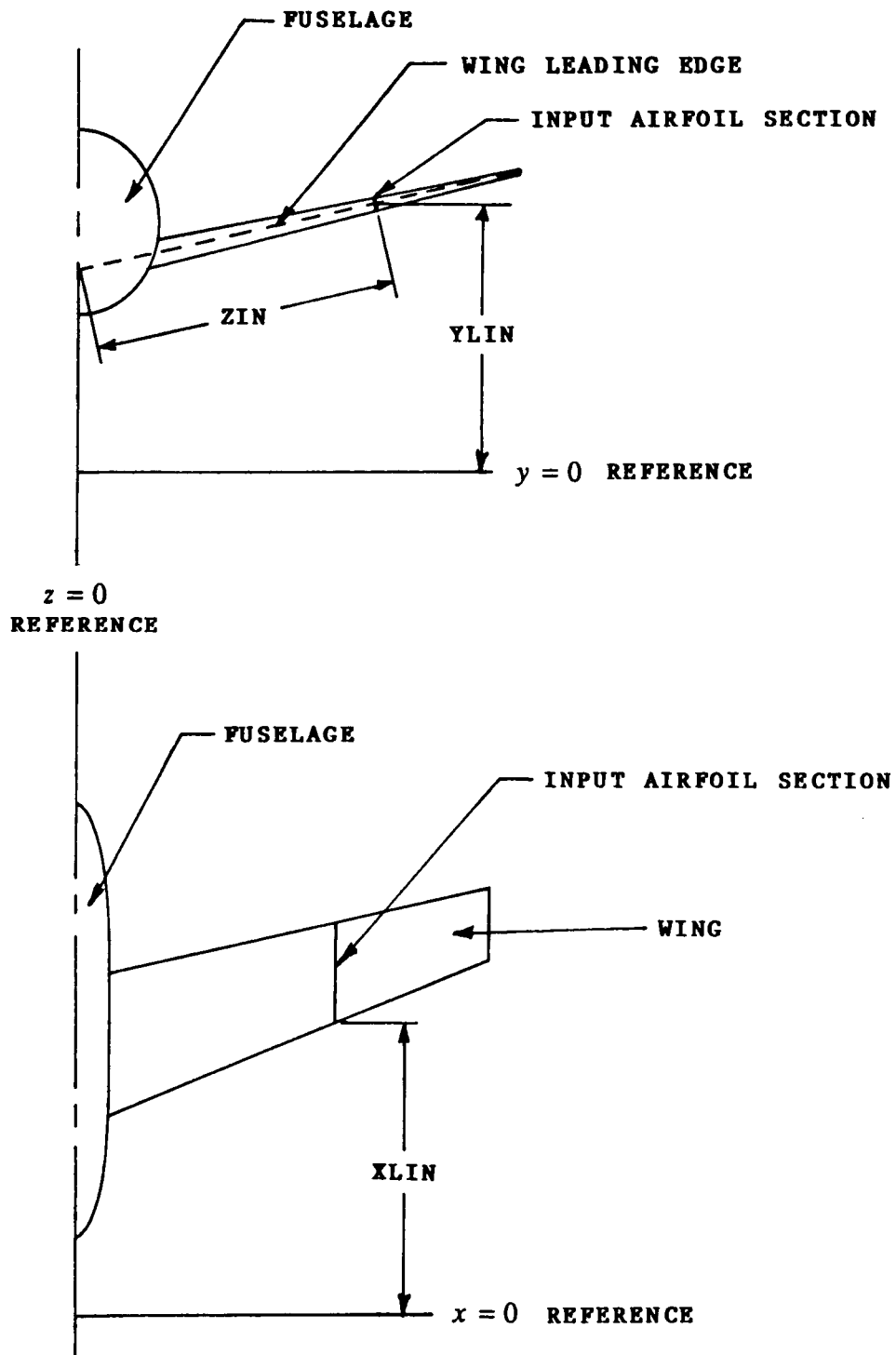


Figure 5. Definition of ZIN, XLIN, and YLIN in read order 5. Dimensions and angles are exaggerated for clarity.



Report Documentation Page

1. Report No. NASA TM-4109	2. Government Accession No.	3. Recipient's Catalog No.	
4. Title and Subtitle Updated Users' Guide for TAWFIVE With Multigrid		5. Report Date May 1989	6. Performing Organization Code
		8. Performing Organization Report No. L-16543	
7. Author(s) N. Duane Melson and Craig L. Streett		10. Work Unit No. 505-60-01-01	11. Contract or Grant No.
		13. Type of Report and Period Covered Technical Memorandum	
9. Performing Organization Name and Address NASA Langley Research Center Hampton, VA 23665-5225		14. Sponsoring Agency Code	
		12. Sponsoring Agency Name and Address National Aeronautics and Space Administration Washington, DC 20546-0001	
15. Supplementary Notes			
16. Abstract A program for the Transonic Analysis of a Wing and Fuselage with Interacted Viscous Effects (TAWFIVE) has been improved by the incorporation of multigrid and a method to specify lift coefficient rather than angle of attack. A finite-volume, full-potential multigrid method is used to model the outer inviscid flow field. First-order viscous effects are modeled by a three-dimensional integral boundary-layer method. Both turbulent and laminar boundary layers are treated. Wake thickness effects are modeled using a two-dimensional strip method. A brief discussion of the engineering aspects of the program is given. The input, output, and use of the program are covered in detail. Sample results are given showing the effects of boundary-layer corrections and the capability of the lift specification method.			
17. Key Words (Suggested by Authors(s)) Viscous-inviscid interaction Three-dimensional wing Transonic flow Multigrid Lift specification		18. Distribution Statement Unclassified—Unlimited Subject Category 34	
19. Security Classif. (of this report) Unclassified	20. Security Classif. (of this page) Unclassified	21. No. of Pages 67	22. Price A04